ASTIA Document No. July 1961

RESEARCH ON SUPER POWER MICROWAVE AMPLIFIER

Report No. 4

Fourth Quarterly Progress Report
1 April 1961 to 1 July 1961

by

H. L. McDowell

S-F-D LABORATORIES, INC.
800 Rahway Avenue
Union, New Jersey

Contract DA 36-039 SC-85379

Department of the Army Task Number 3A99-13-001-05

U. S. Army Signal Research and Development Laboratory
Fort Monmouth, New Jersey

This contract is sponsored by the Advanced Research Projects Agency
under ARPA Order No. 130-60, Project Code No. 7800

ASTIA Document No.

July 1961

RESEARCH ON SUPER POWER MICROWAVE AMPLIFIER

Report No. 4

Fourth Quarterly Progress Report

1 April 1961 to 1 July 1961

by

H. L. McDowell

Approved by

J. Feinstein

S-F-D LABORATORIES, INC.
800 Rahway Avenue
Union, New Jersey

Contract DA 36-039 SC-85379

Department of the Army Task Number 3A99-13-001-05

U. S. Army Signal Research and Development Laboratory
Fort Monmouth, New Jersey

This contract is sponsored by the Advanced Research Projects Agency
under ARPA Order No. 130-60, Project Code No. 7800

TABLE OF CONTENTS

PURPOSE

The purpose of this contract is to conduct research on crossed-field amplifiers in accordance with Technical Guidelines MW-21, a copy of which is included in the first quarterly report.

PUBLICATIONS, LECTURES, REPORTS AND CONFERENCES

1. Meeting at S-F-D laboratories to discuss contract, April 21, 1961. Mr. J. D'Andrea, I. Reingold, K. Garoff of the Signal Corps and J. Feinstein and H. L. McDowell of S-F-D laboratories were present.

2. Classified conference on Super Power Tube Program at Lincoln Laboratories, Massachusetts Institute of Technology, April 25 - 26, 1961. J. A. Saloom, J. Feinstein and H. L. McDowell of S-F-D laboratories attended. J. Feinstein presented a review of the S-F-D laboratories' program.

ABSTRACT

During this quarter construction of the first SFD-203 tube has been completed. The tube is now being pumped. Experiments on the SFD-202 and SFD-205 have shown that frequency responses flat over 8 - 12% bandwidth can be obtained with constant anode voltage. Experiments on a smooth bore tube have shown that the frequencies of the space charge mode are largely determined by a coaxial line resonance of the stem. Experiments on the SFD-202 have shown that control electrode turn-off can be accomplished with a geometry which is compatible with our usual techniques for debunching spokes in the drift region.

1.0 INTRODUCTION

During this quarter, the SFD-202, SFD-203, SFD-205 and SFD-207 programs have all been carried forward. A complete SFD-203 tube has been constructed, cold tested and is presently being pumped. Tests on the SFD-205 have yielded promising results. In one experiment we obtained 16 db of gain with 400 kw output and 13 db of gain with 700 kw output. In another experiment we obtained about 13 $\pm$ 0.75 db gain at about 300 kw output over the 8.5 to 9.6 kMc band with efficiencies as high as 59%. Tests on the SFD-207 have not been as successful. We have obtained about 150 kw output with 8 db of gain and 25% efficiency. We are presently trying to understand the reasons for the differences in performance of these two tubes.

As part of the SFD-202 program, we have made further experiments with a smooth-bore tube. These experiments have shown clearly that the smooth-bore mode frequencies are tied to resonances of the interaction space and specifically, that the frequencies observed in the 2 kMc range are related to a TEM mode in which the stem is resonating in a $\lambda/4$ mode. Experiments are now being prepared to investigate the effect of damping these modes.

On the SFD-202 itself, we have carried further the experiments on turn-off using a control electrode and have demonstrated such turn-off in a configuration more practical than the one discussed in the last quarterly report. Several experiments on controlling the space charge mode were tried with negative results.

Off and on, we have been troubled with multipactor effects in our tubes. Some attention was given to this problem during the past quarter. At least a partial understanding of the effect was obtained. It appears that multipactoring along a vane surface under the influence of crossed RF electric and dc magnetic fields is the major source of our trouble.

Problems with our beryllium copper cathodes have begun to show up at X-band - the main symptom being deactivation of the cathodes after arcs have been drawn. After such deactivation, we run into the maximum current boundary phenomenon described by Jepsen and Muller. It appears that a tube operates satisfactorily as long as the maximum current boundary has not been exceeded and the tube is space charge limited. If we try to draw currents greater than this, the tube ceases to operate and the current drops to a low value. Thus, these tubes will apparently not operate at all under emission limited conditions.

2.0 THE SFD-203 PROGRAM

The first complete SFD-203 tube was constructed during this quarter. It is presently being pumped and prepared for RF test. Figure 1 shows a photograph of this tube. A cathode height of 0.250 inch is employed rather than the 0.4 to 0.5 called for in the initial design to lower the current drawn to within the capabilities of our hard tube modulator. A control electrode will be tried in this tube and, if successful, the next experiment will be performed using the full height cathode and a dc power supply. No attenuation is incorporated in this first tube.

Cold tests on this tube showed an insertion loss of about 3 db with some additional dips to 4 to 5 db loss. These dips are most likely due to resonances of the large can structure in which the circuit is mounted. We decided to temporarily bypass this problem since there are frequencies within the band at which the tube can be satisfactorily tested. In this manner, we can get hot test data most quickly and, thereby, see if any major problems show up. Figure 2 shows results of the cold test measurements.

We can make a quick calculation to see how reasonable the 3 db insertion loss is compared to an ideal figure for an array of half-wave wires. From Pierce[1] we find

$$\alpha = 27.3 \left(R/\sqrt{\mu/\epsilon}\right) (c/v_g)\, N$$

where
- R = the surface resistivity of the circuit material
- $\sqrt{\mu/\epsilon}$ = 377 ohms, the intrinsic resistance of space
- c = the velocity of light
- v_g = the group velocity of the circuit
- N = the number of wavelengths along the circuit.

FIGURE 1 - PHOTOGRAPH OF THE SFD-203

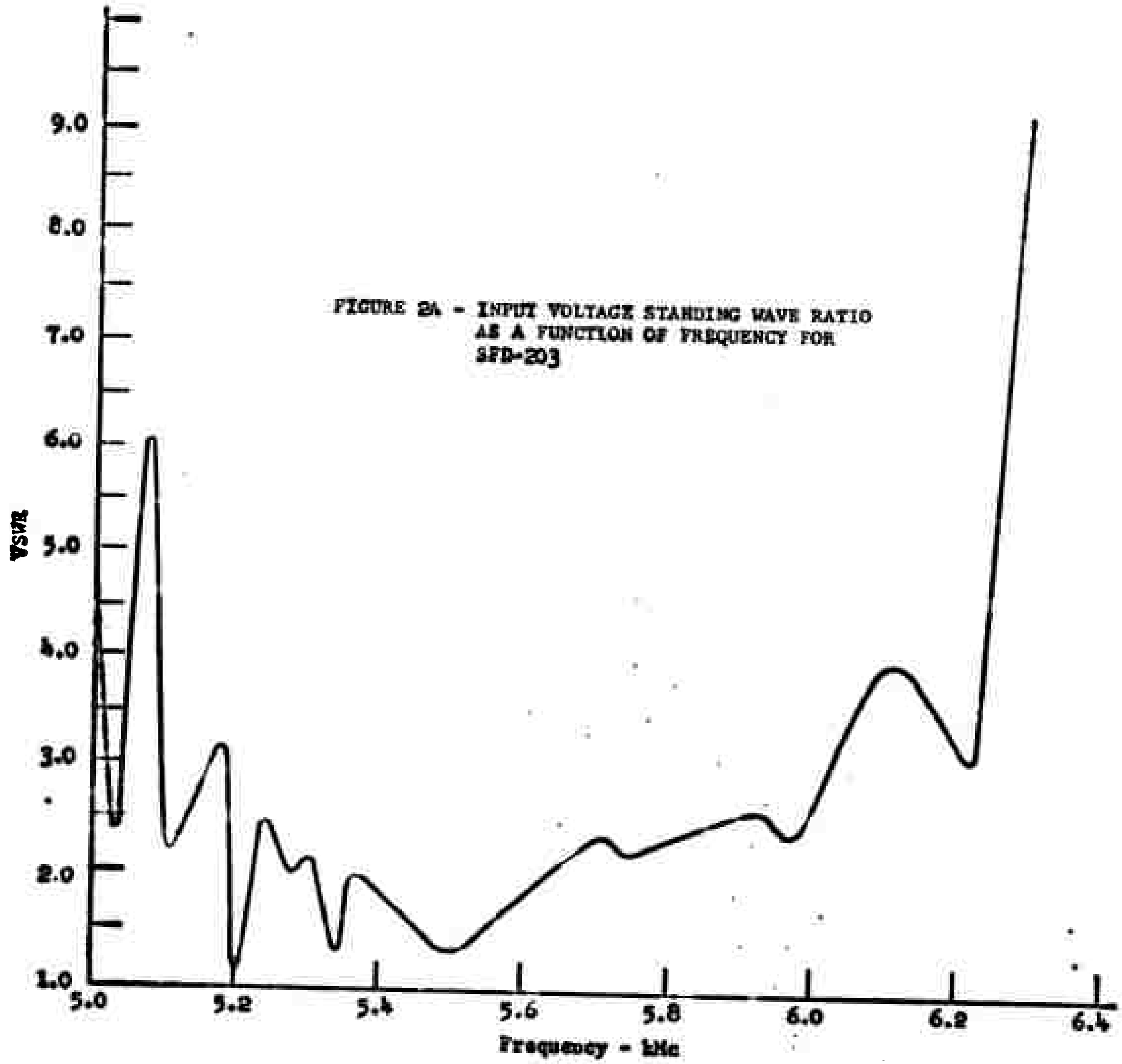

FIGURE 2A - INPUT VOLTAGE STANDING WAVE RATIO AS A FUNCTION OF FREQUENCY FOR SFD-203

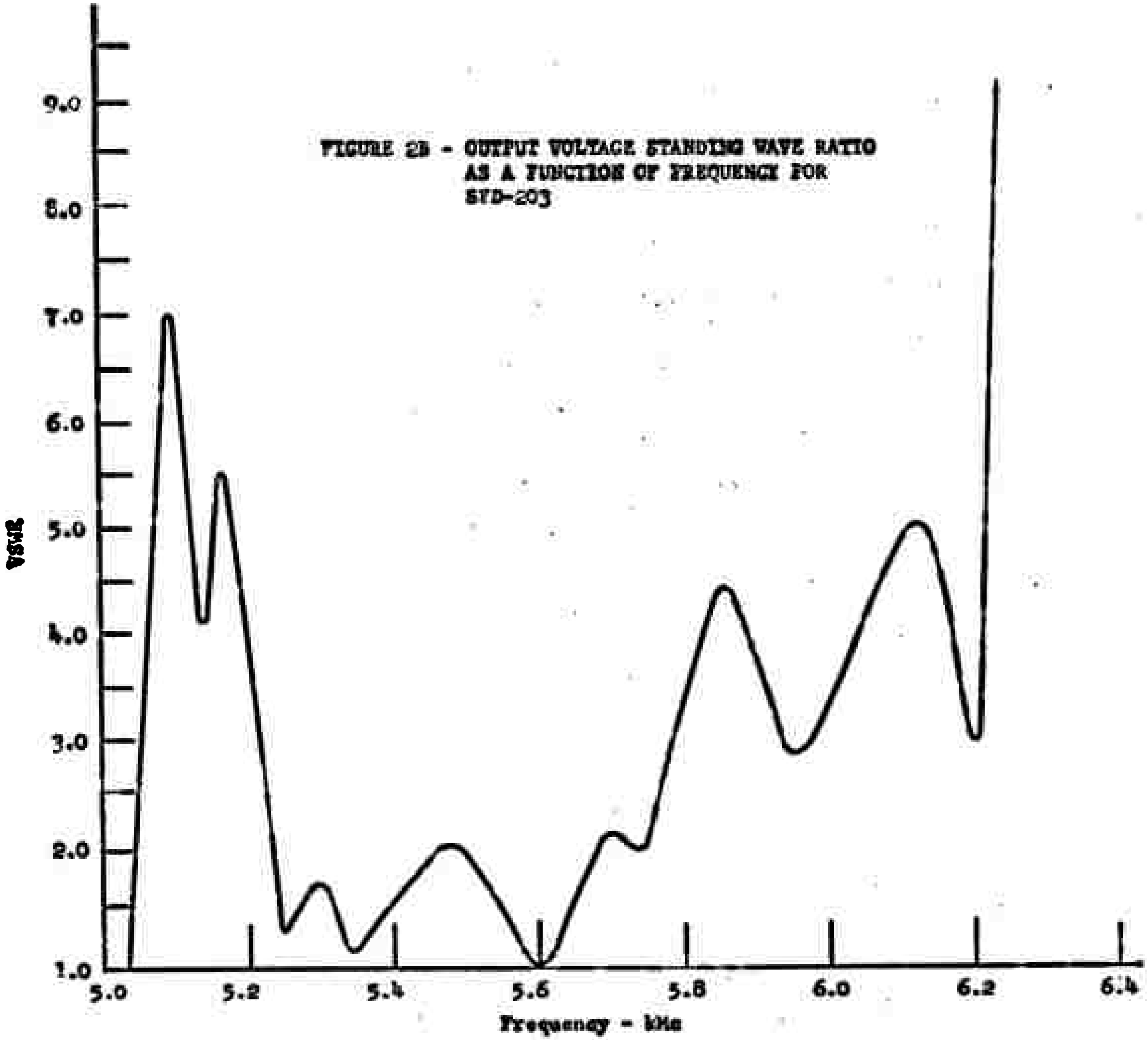

FIGURE 2B - OUTPUT VOLTAGE STANDING WAVE RATIO AS A FUNCTION OF FREQUENCY FOR STD-203

Taking the synchronous voltage as 3 kv, the ratio $v_g/v_p = 0.5$, and $N = 30$ wavelengths, we find for a copper circuit allowing a factor of 1.2 in R for surface roughness

$$\alpha \approx 1.0 \text{ db}$$

The discrepancy between this ideal value and the 3 db measured is accounted for by the finite size of the bars, loss in the C_{13} couplers which is not included in the above calculation and loss in the input and output circuits. We estimate that with care these losses might be reduced until we have a total circuit loss of about 2 db.

3.0 SMOOTH BORE EXPERIMENTS

3.1 Small Diameter Smooth-Bore Tube

It will be remembered from our third quarterly report that a rather confusing picture was emerging with regard to the frequencies at which smooth-bore modes occurred. Much of the energy appeared to be centered around 2 kMc and was not changed from this location when varying the anode-to-cathode spacing. Sometimes tunable oscillations were encountered; sometimes the oscillations appeared to stick at certain frequencies. When the same demountable smooth-bore tube was put together with a 0.910 diameter cathode on two separate occasions, different results were obtained.

During the past quarter an experiment was performed which has shed considerable light on this situation. In this experiment, an insert was placed within the anode of the smooth-bore tube to reduce the anode diameter to 0.400. An 0.250 diameter cathode was used, thus maintaining the anode-to-cathode spacing about the same as in our original experiments. The purpose of this experiment was to see if the frequency of the space charge modes scaled up in proportion to the anode size reduction. With the new small cathode geometry, there was no longer room for a hot button in the cathode. We had previously ascertained, however, that the smooth-bore tube could be started by applying an input pulse of several kilowatts to one of the coaxial probes. We thus decided to use this method of starting. The coaxial probes themselves had to be redesigned to a smaller size to fit in the new geometry. Thus, the whole geometry of the tube was essentially changed.

When this tube was tested, two interesting features appeared. One of these was the maximum current boundary phenomenon; the other was the fact that the space charge mode frequencies had remained at 2 kMc in spite of all our changes. The maximum current boundary phenomenon is illustrated in Figure 3 where we show current as a function of the ratio

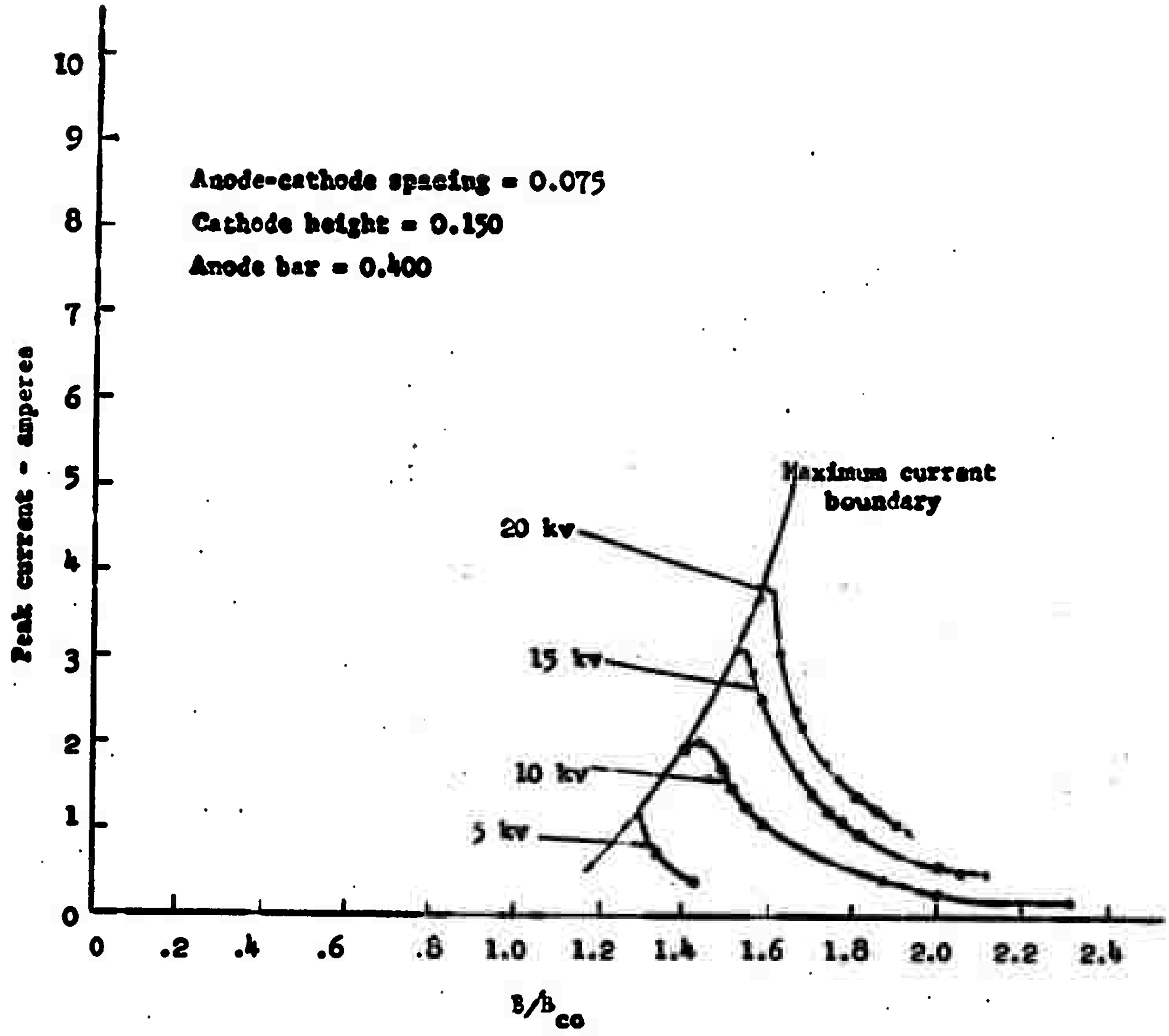

FIGURE 3 - CURRENT AS A FUNCTION OF THE RATIO OF MAGNETIC FIELD, B, TO THE CUT OFF VALUE OF FIELD, B_{co}, FOR DIFFERENT ANODE VOLTAGES

of the magnetic field to the cut-off field. The current increases as field is decreased until a sharp boundary is reached and the current drops to zero. We found that the location of this boundary was insensitive to the input power used to trigger the space charge mode over a five-to-one range from minimum power which would trigger the tube to the maximum available. This indicates that the boundary is not related to the starting process. (The current drawn in this experiment was measured after termination of the input RF trigger pulse)

The area of the cathode in this experiment is 0.275 times the area used in the previous smooth bore experiments. The current for a given B/B_{co} is however much larger than 0.275 of that drawn from the larger diameter smooth-bore tube. This is shown in Figure 4 where the results for the small diameter tube are compared with those for the large diameter tube as taken from Figure 11 of the third quarterly report. It would appear that the greater curvature of the small tube has enhanced the space charge mode rather than reduced it as we once suspected. It will also be noted from Figure 4 that the maximum current drawn from large and small diameter tubes is about the same. This must be in part a matter of coincidence because in the large diameter tube cut-off is reached before we reach a maximum current boundary; whereas in the small diameter tube, a clearly defined maximum current boundary is found for fields higher than cut-off. Thus in the large diameter tube, the current is limited by electronic effects while in the small diameter tube it is apparently limited by the maximum current the cathode is capable of delivering. The reason for these differences in performance of large and small diameter tubes is not presently understood.

Figure 5 shows the spectra of the smooth-bore oscillations as obtained from the small diameter tube under several different operating conditions. As may be seen, there are a group of frequencies near 2 kMc and another near 5 kMc. The 2 kMc oscillations would not tune, but those at 5 kMc would tune with magnetic field over a narrow range. The tube was next cold checked for transmission between the two coaxial probes.

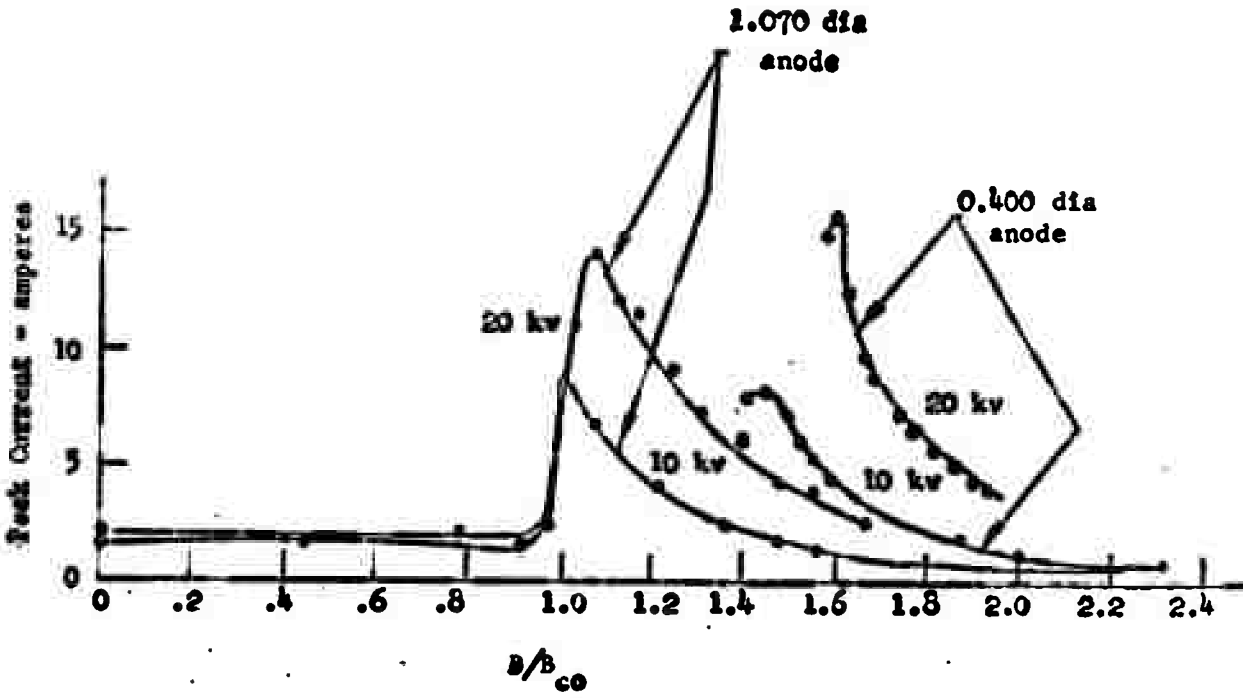

FIGURE 4 - COMPARISON OF CURRENT vs B/B_{co} FOR 0.400 and 1.070 DIAMETER SMOOTH-BORE TUBES

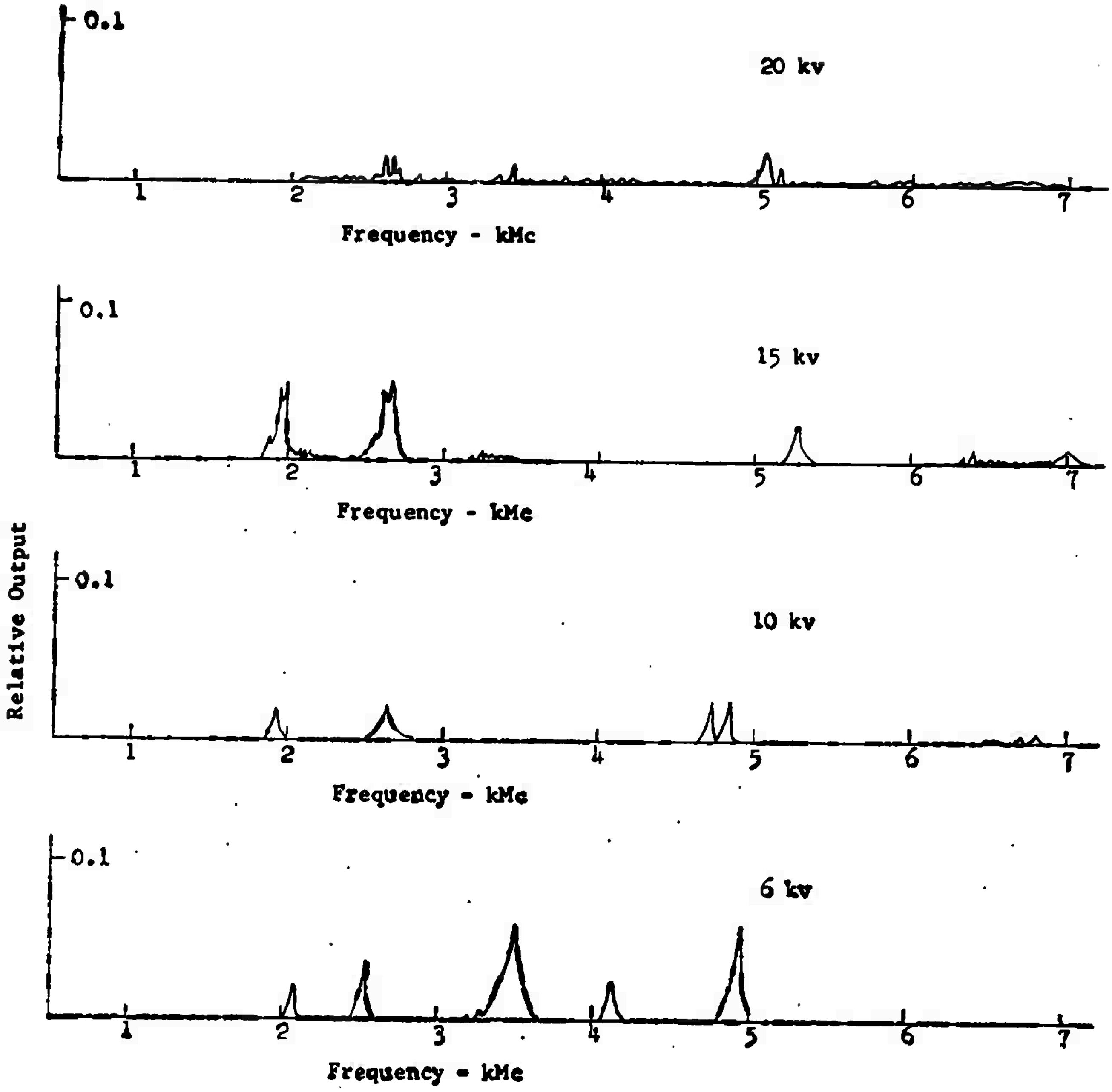

FIGURE 5 - SKETCHS OF SPECTRA OBSERVED IN 0.400 DIAMETER ANODE SMOOTH-BORE TUBE AT DIFFERENT VOLTAGES

A group of resonances was detected in the 2 to 4 kMc range though no resonances were found near 5 kMc. It thus seems extremely likely that the smooth-bore mode frequencies - at least those between 2 and 3 kMc - are tied to circuit resonances. It is likely that those near 5 kMc are also tied to a resonance but that we missed the resonance on cold test. We tentatively advance the conclusion that the space charge mode phenomenon is an extremely broadband one and that the exact frequency that it picks to operate is determined by whatever resonances may be present. This conclusion is further justified by the observation that tuning the output line through which these modes are observed also causes shifts in their frequencies. A lower limit to the frequencies permitted is obtained when the walls of the interaction space short out the RF fields of the space charge mode between regions of electron bunching and regions of electron deficiency. In our case this appears to be about 1 kMc. An upper boundary to the permitted frequencies appears to be the cyclotron frequency.

It was next noted that the frequency of 2 kMc corresponded roughly to that at which the cathode stem was a quarter wavelength long. Further experiments did indeed show that the observed resonances are TEM modes in which the stem acts as a quarter wave coaxial resonator. Such resonances were observed on a stem assembly alone removed from the tube.

The next obvious step is to find out what happens when the resonances of the interaction space are damped out. It is our suspicion that the space charge mode will continue to draw current but that it will generate a broad spectrum of noise. To check this, we are now constructing a smooth bore experiment in which a carbon loaded ceramic absorber is used as the anode. This will be done using the large smooth bore geometry. The dc resistance of the absorber is low enough so that there will be only a few hundred volts drop between its face where the electrons are collected and the metal surface on which it rests.

3.2 Electronic Gain in a Smooth-Bore Tube

During some experiments on the standard size smooth-bore tube (1.070 inch diameter anode, 0.910 inch diameter cathode), it was observed that not only will an RF signal trigger the smooth bore on with the cathode running completely cold (hot button turned off) but that this signal will experience electronic gain; i.e., the coupling loss between probes is reduced. Net gain between probes was never obtained but the coupling loss was decreased by a factor of 10 db. The amount of electronic gain was greatest when the polarity of the magnetic field was such that the electrons traveled the short distance between probes - see Figure 6A. As magnetic field was varied, there were a series of variations in gain and a greater number of variations in starting time delay.

It would appear that the electronic gain is a crossed-field klystron like effect since the gain is greatest for the shortest path length of the electrons between probes. Apparently, the electrons become velocity modulated under the input probe and this velocity modulation is converted either to displacement or density modulation under the output probe. As the magnetic field is changed, the optimum drift length changes. This may account for the power output variations. If the electrons have to go the long way around the tube between input and output probes, the modulation evidentally decays and the electronic gain is less. If on the other hand the gain mechanism were a diocotron like mechanism such as we suspect for the space charge mode, we would expect that the gain would be higher the long way around the tube if there were any difference at all. Thus the effect we see is not likely to be a diocotron effect and may be unrelated to the space charge mode phenomenon.

Starting time delay in this experiment may have to do with the phase at which electrons return under the input probe after a single transit around the tube. The number of minima in starting time delay as a function of magnetic field appears to be about four times the number of

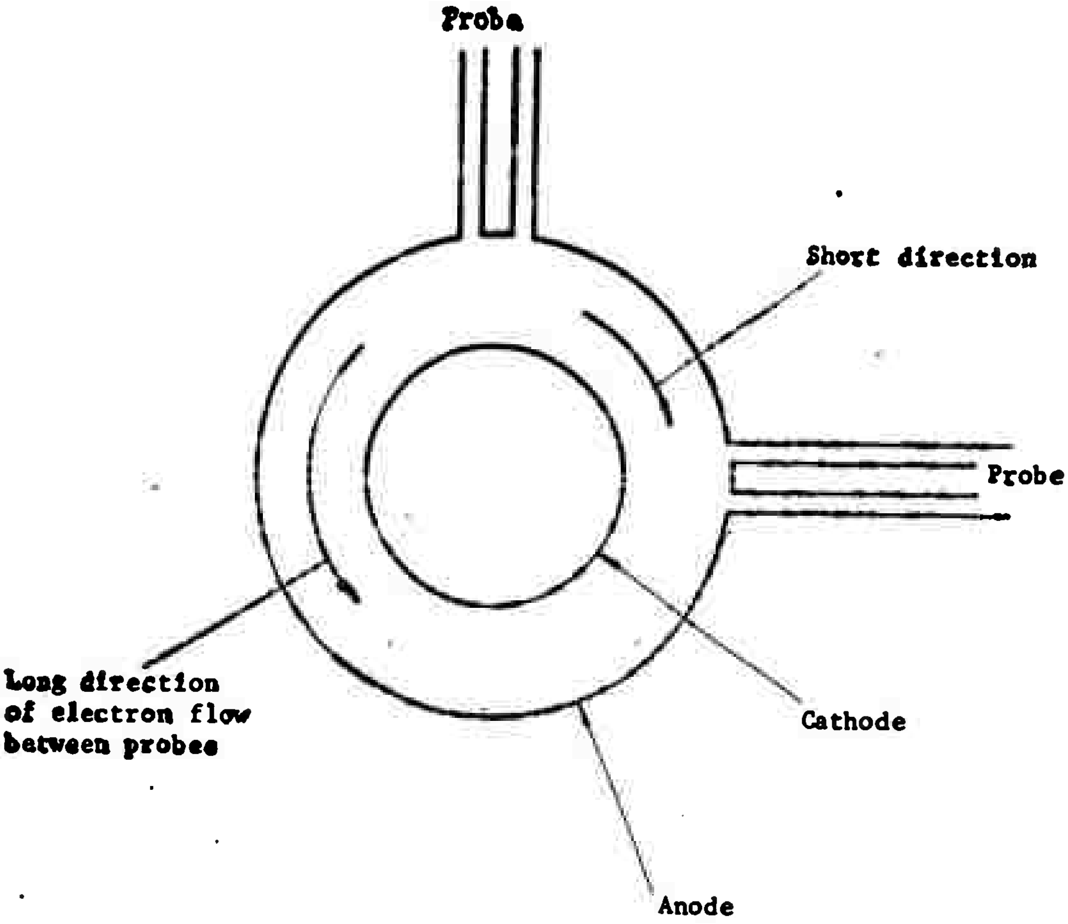

FIGURE 6A - SKETCH SHOWING WHAT IS MEANT BY SHORT AND LONG DIRECTIONS OF ELECTRON FLOW BETWEEN PROBE POSITIONS wiggles in the electronic gain curve. Thus it would appear likely that the starting time delay variations are related to transit time all the way around the tube while variations in electronic gain are related to transit time between probes; i.e., a quarter of the way around the tube.

3.3 Present View of Space Charge Mode

In our second quarterly report, we started an analysis of the smooth Brillouin hub in a crossed-field tube with a continuously emitting cathode. This analysis is essentially Buneman's[2]. It shows that there may be a mechanism for hub instability where $\omega > \omega_c$ but experimentally we do not observe this and $\omega < \omega_c$ for all our space charge modes. In the region of $\omega < \omega_c$ we find an inverted reactance characteristic looking into the electron cloud. If this is loaded with a positive conductance, hub surface instabilities can occur. With perfectly conducting walls, the hub should be stable. In the second quarterly report we speculated that the finite conductivity of the walls might give rise to a slight net gain and if the hub went around the tube enough times, this small gain over a long distance might be enough to account for the hub break up.

During the third quarter an experiment was performed which appears to show this explanation to be incorrect. As described in Section 4.3 of the third quarterly report, an experiment was conducted in which the re-entrancy of the electrons was eliminated by a collector in the drift space of a tube and electrons were started off near the input from a hot cathode button. This tube drew current as a result of a space charge mode thus indicating that the gain mechanism of this mode is high enough for the mode to build up to appreciable amplitudes for a single transit of the electrons around the hub. Thus, it appears that we have to look for a higher gain effect than any we can derive from a Brillouin hub. Such a gain effect can be postulated if we look at the striated solutions for the hub space charge as described for example in Slater[3].

In such solutions the space charge distribution and electron trajectories appear as sketched in Figure 6B. The outer rim of space charge in this solution begins to look a bit like the strip beam in an injected beam crossed-field tube. It is thus quite possible that the outer rim can support waves on both its top and bottom surface and that these can couple giving rise to diocotron gain. Another way of saying this is that the rim may be unstable with respect to bowing along the direction of travel whereas the Brillouin hub is not. Thus it may well be an instability of the striated solution that gives rise to the space charge mode rather than an instability of the lowest order or Brillouin solution of the hub. At present this looks to us like the most reasonable explanation for the space charge mode.

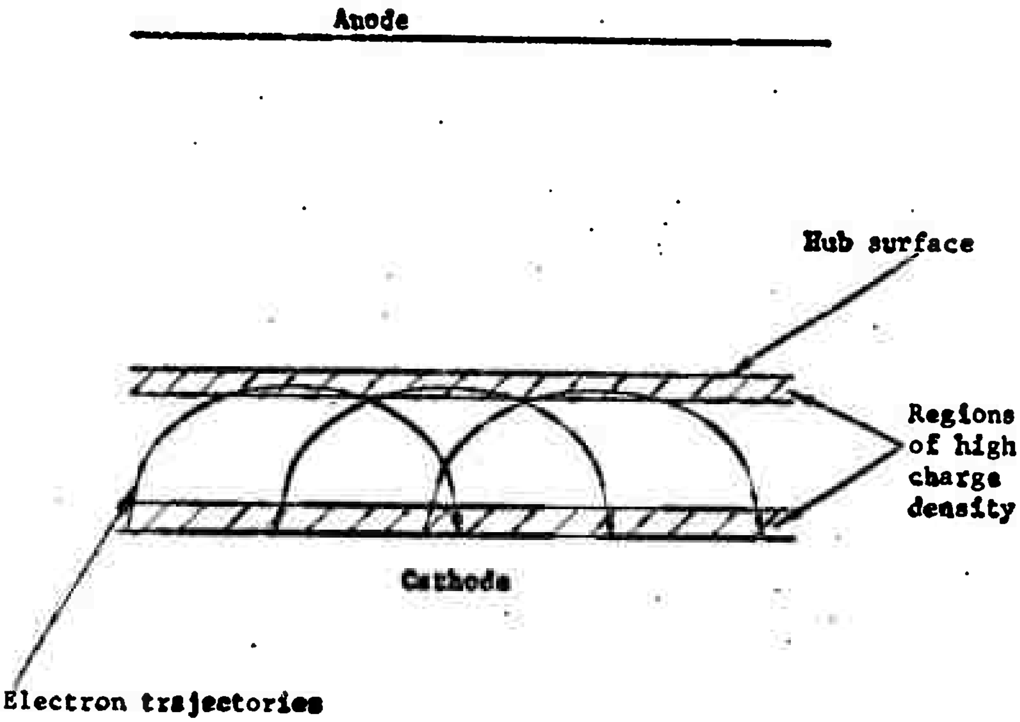

FIGURE 6B - SKETCH OF STRIATED SPACE CHARGE IN HUB

4.0 THE SFD-202 PROGRAM

4.1 Experiments on Turn-off using a Control Electrode

In the last quarterly report we discussed a method of turning off a crossed-field amplifier by pulsing a segment of the cathode positive with respect to the main cathode. This segment then collected the circulating current and caused turn-off. The segment used in this case constituted one-third of the cathode circumference. During the past quarter, we have performed further experiments on control electrodes in an attempt to get a configuration that would fit wholly within the drift space.

The first experiment tried used a control electrode configuration as shown in Figure 7A. With a dc voltage of 15 kv, a 3 kv pulse positive with respect to the cathode gave turn-off. With less than a 3 kv pulse, turn-off was not obtained. There was a sharp demarcation between the pulse voltage required for turn-off and that which would not give turn-off. Thus, the mu for this configuration is 5.

In the second experiment we used the configuration shown in Figure 7B. This configuration combines the control electrode with our normal drift section geometry. We were not able to get a complete test of this configuration because the tube was damaged by an arc drawn from end hat to pole piece. Before arcing the tube was operating satisfactorily with a 4.5 kv control electrode pulse. No attempt had been made up to this time to lower the control electrode voltage below 4.5 kv. We are presently preparing to repeat this experiment with increased end hat to pole piece spacing to reduce arcing.

4.2 Complete Interruption of the Drift Space

In Section 4.3 of the last quarterly report we discussed an experiment in which the drift space was completely interrupted and a hot cathode button was used near the input. This tube operated in a space charge mode in spite of the interruption of the electronic feedback.

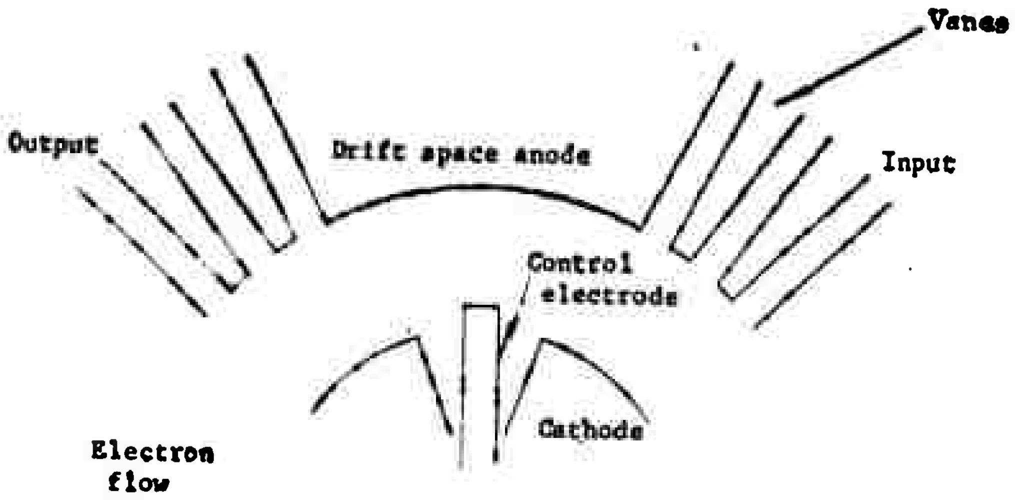

FIGURE 7A - SKETCH OF CONTROL ELECTRODE GEOMETRY IN WHICH A CONTROL ELECTRODE PROTRUDES FROM CATHODE IN DRIFT SPACE

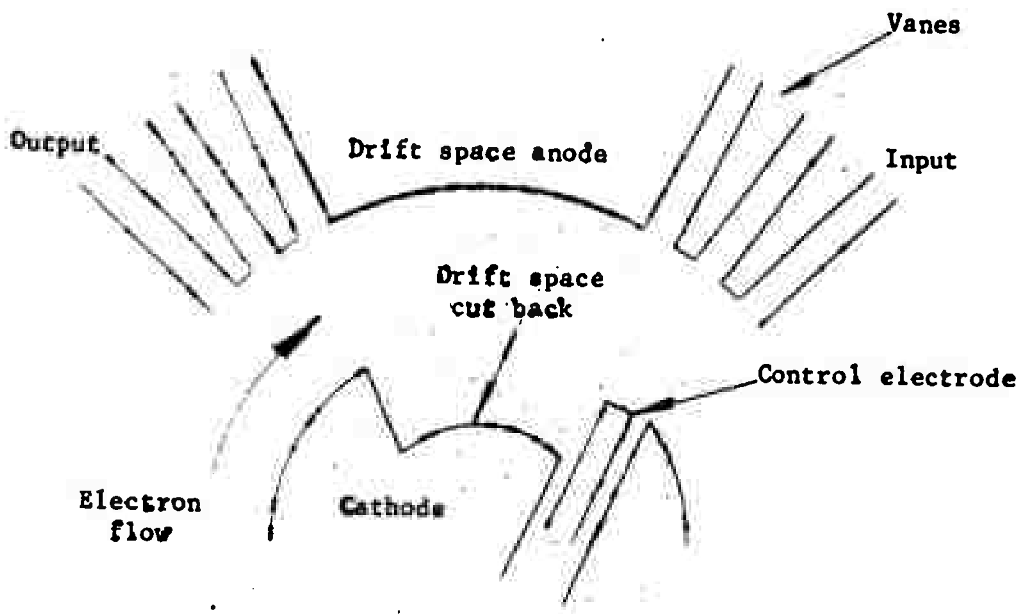

FIGURE 7B - SKETCH OF CONTROL ELECTRODE GEOMETRY IN WHICH CONTROL ELECTRODE IS MOUNTED AT END OF CATHODE CUT-BACK SECTION IN DRIFT SPACE

During the past quarter we repeated this experiment with an absorber mounted directly on the top of the vanes of the circuit. The purpose of this experiment was to see if we could damp out the space charge mode by eliminating its means of feedback, believed to be fast RF wave in this case. Experimentally, we found the space charge mode unaffected by this absorber. We know now as a result of the experiments on the smooth-bore tube discussed above, that a major source of feedback may be a TEM mode resonance near 2 kMc. This mode would not have been much affected by the absorber on the vanes.

4.3 Experiments on Grid Wires in the Drift Space

Several experiments were tried with grid wires mounted circumferentially in the drift space as sketched in Figure 8. These wires were mounted on a support separate from the cathode so that they would be biased positive with respect to the cathode. It was intended that the wires be located just outside the hub and operate at the normal hub surface potential. It was thought that the wires might short out the RF field of the space charge mode in the drift space and thereby prevent its operation.

The inclusion of this grid was a difficult mechanical problem and several false starts were made before a successful test was made. The results were that the grid does not reduce the space charge mode and that it is difficult to avoid intercepting a large current on the grid thereby lowering efficiency. This type of grid appears to be an unpromising approach for control of space charge modes and experiments on it will not be carried further.

4.4 Quadded Anode Tube

A tube was constructed and tested having an anode in which the size of the slots between vane resonators and serpentine line were varied in groups of four from 45 mils to 25 mils; i.e., the first four slots of the circuit would be 45 mils wide, the next four 25 mils wide, etc. This

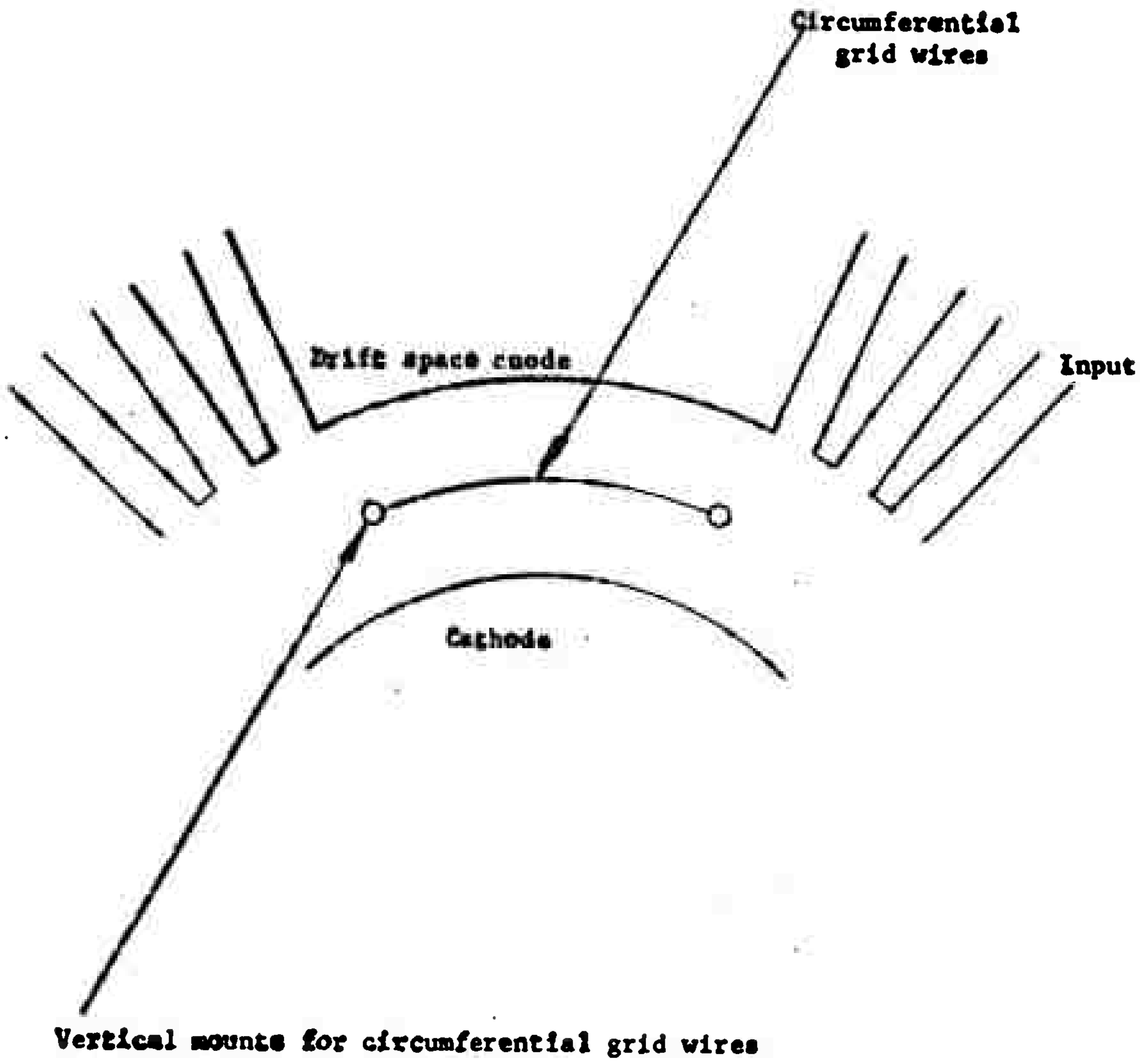

FIGURE 8 - SKETCH SHOWING LOCATION OF CIRCUMFERENTIAL GRID WIRES IN THE DRIFT SPACE

technique is known as quadding. In coaxial magnetrons it has been a strong tool in eliminating moding. In our case we believed that a possibility existed of reducing the spurious noise near the π mode by quadding. Tests showed however that the quadding had practically no effect on performance.

4.5 Experiments on Leakage Current

To determine how much leakage current was drawn from the interaction space to the pole piece, we constructed a cover for our demountable SFD-202 tubes having the pole face insulated from ground by a thin ceramic wafer. A separate lead was brought out from this insulated pole face so that we could monitor the leakage current. The effect of insertion of the insulating wafer on magnetic field was checked and found to be negligible.

This cover with insulated pole face was used to check leakage current in two separate experiments on the SFD-202. In both cases, the measured leakage current was found to be very low - amounting to no more than 2-1/2% of the total current at low magnetic fields and no more than 1% at normal operating field. Assuming that an equal leakage current was drawn to the lower pole piece, the total leakage current amounts to 2 to 5% of the cathode current. This means that essentially all the cathode current goes directly across to the anode even when the magnetic field is low enough so that the hub surface extends beyond the end hat radius. Prior to this experiment the possibility seemed to exist that some of the large current drawn at low ratios of B to B_{co} was leakage to the pole pieces. This experiment shows that leakage effects are negligible.

4.6 Frequency Response of the SFD-202

The frequency response of the SFD-202 was measured with a constant 3 kw input drive at three different values of magnetic field. Figure 9 shows the results. At high magnetic fields the output slopes upward toward the lower frequencies. The slope of the curve represents

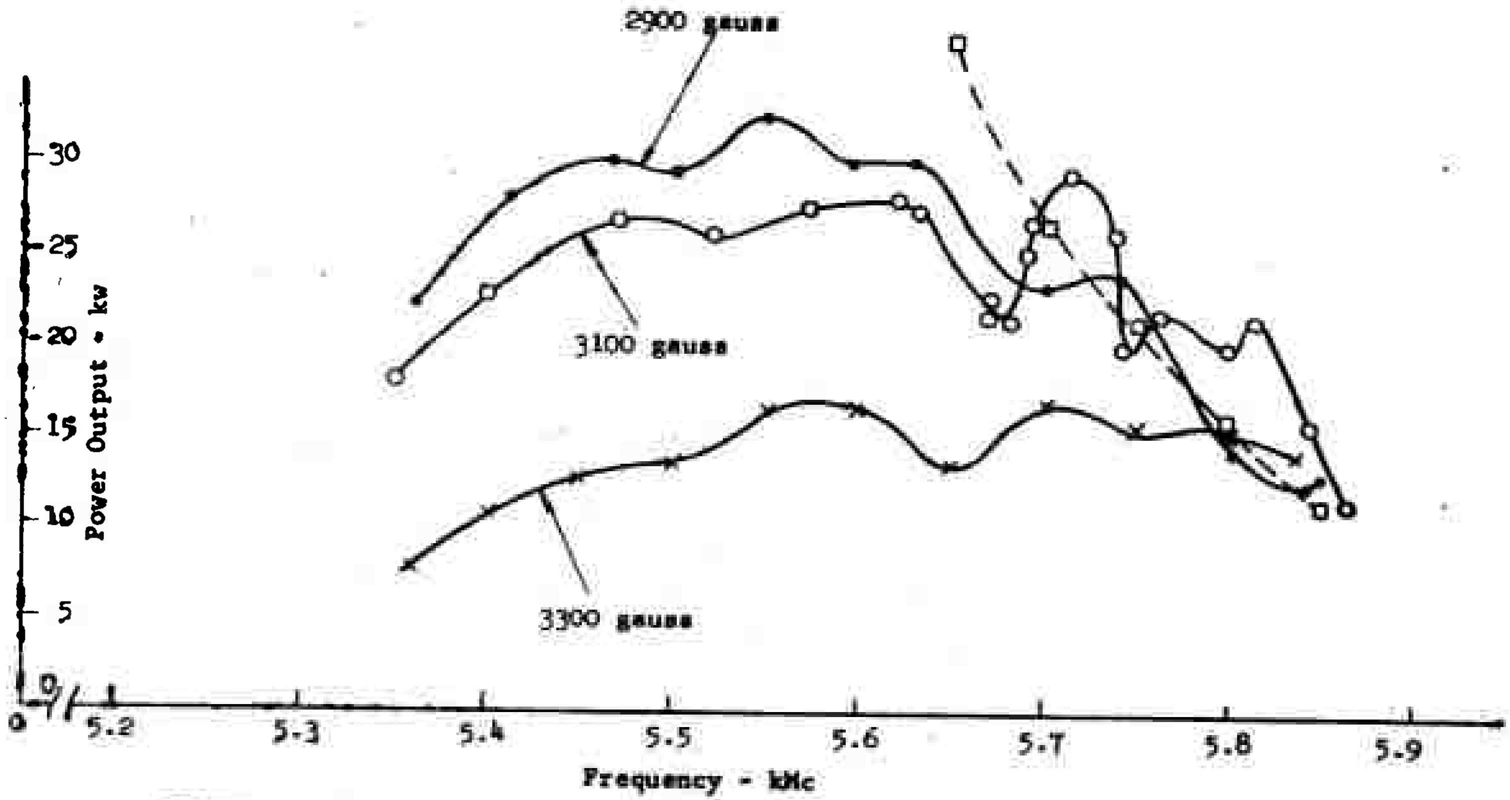

FIGURE 9 - POWER OUTPUT AS A FUNCTION OF FREQUENCY FOR THE SFD-202 AT VARIOUS MAGNETIC FIELDS AND A FIXED INPUT POWER OF 3 kw.

a compromise between two effects - the magnitude of the field at the hub surface and the ratio of anode voltage to the Hartree voltage. At low frequencies, the rate of decay of the RF fields away from the circuit is less rapid and the RF field at the hub surface is stronger than at high frequencies. This tends to make the tube draw a higher current and causes the gain to be higher at the low frequency end of the band. On the other hand for fixed voltage and magnetic field, the percentage over-voltage is larger at the upper end of the band as may be seen from the sketch of Figure 10. By proper choice of magnetic field for a given voltage (or vice versa) these two effects can be made to balance and the average slope removed from the frequency response curve.

The wiggles in the curve of Figure 9 are believed to be related to circuit reflections. This curve covers a range over which the feedback caused by electrons not being completely debunched in the drift space would alternate several times from positive to negative. The absence of such periodicity in the frequency response indicates that such feedback is small.

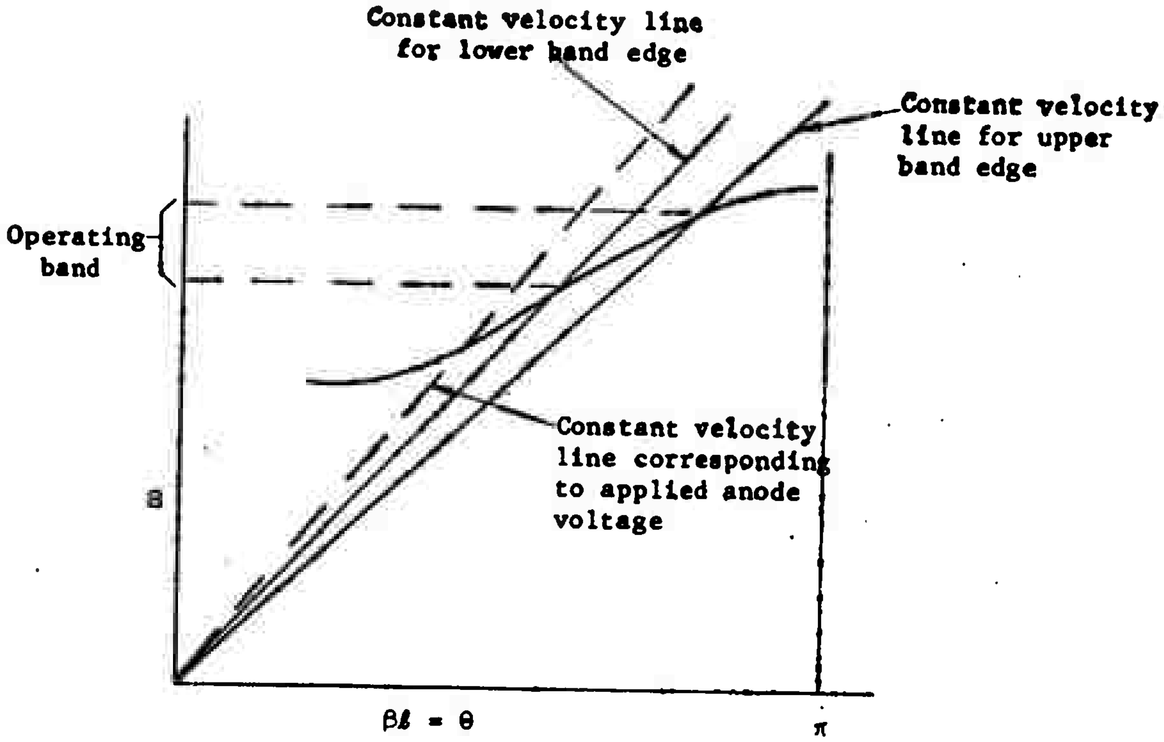

FIGURE 10 - SKETCH SHOWING HOW CONSTANT VELOCITY LINE INTERSECTS ω-β PLOT. THE PERCENTAGE OF VOLTAGE ABOVE THE HARTREE VALUE IS GREATER AT THE UPPER END OF THE BAND THAN AT THE LOWER END

5.0 THE X-BAND PROGRAM

5.1 The SFD-205

The SFD-205 is an X-band serpentine line tube similar in principle to the SFD-202. It is a higher power tube than the SFD-202 and operates at a higher synchronous voltage thus making the spacings in the serpentine line greater than in the SFD-202. We consider the design of the SFD-205 to be a "practical one" whereas we do not so consider the SFD-202 design. From tests on this tube we expect to get a clearer understanding of the operation of a forward wave crossed-field amplifier at this moderate gain (15 db) level. This will assist us later in interpreting results on the higher gain SFD-203.

The first extensive testing of the SFD-205 has been conducted during this quarter. One major problem has shown up - the beryllium copper cathodes tend to deactivate after arcing has occurred in the tube. This problem will be discussed further in the section on cathodes. A second problem has been a tendency to multipactor. This problem is also discussed below. In spite of these difficulties some very interesting results have been obtained. Figure 11 shows a scatter of points taken at different magnetic fields and voltages on a plot of power output as a function of power input. It is seen that gains as high as 17 db and power outputs as high as 700 kw were obtained. These results were obtained in an early test in which the anode was loaded heavily by an absorber so that transmission was obtained only over a narrow bandwidth. This was necessary because the end slots of the circuit were radiating giving rise to a very ragged bandpass characteristic unless the absorber was used.

In subsequent cold tests the radiation problem was cured by putting shorts part way up the first and last slots. The bandpass characteristic then looked relatively good over the 8.5 to 9.6 kMc band.

A hot test performed on this tube gave the results shown in Figure 12. A relatively flat curve was obtained with 12 to 13 db of gain.

FIGURE 11 - POWER OUTPUT AS A FUNCTION OF POWER INPUT FOR THE SFD-205. DIAGRAM SHOWING A SCATTER OF POINTS TAKEN DURING INITIAL MEASUREMENTS

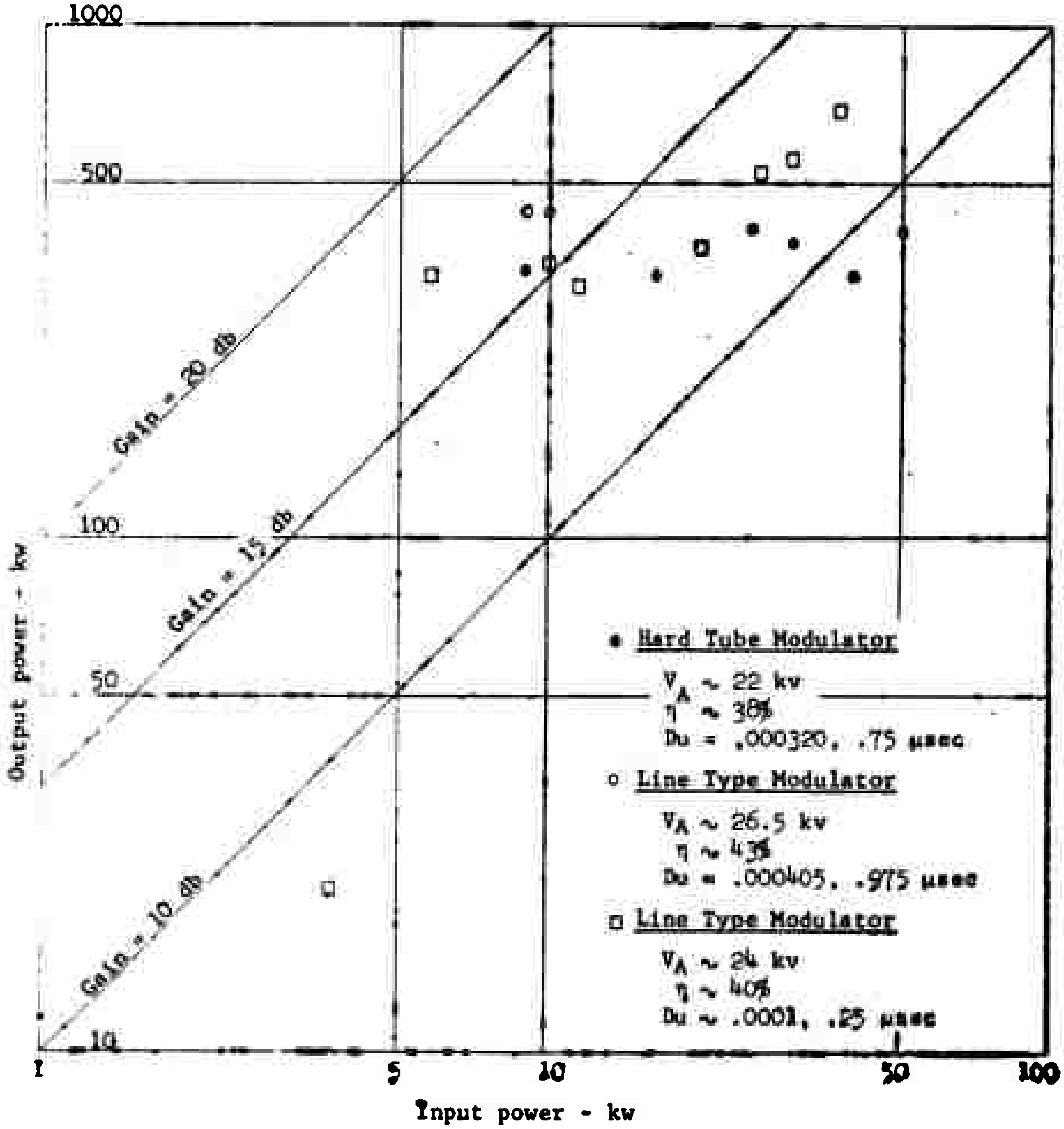

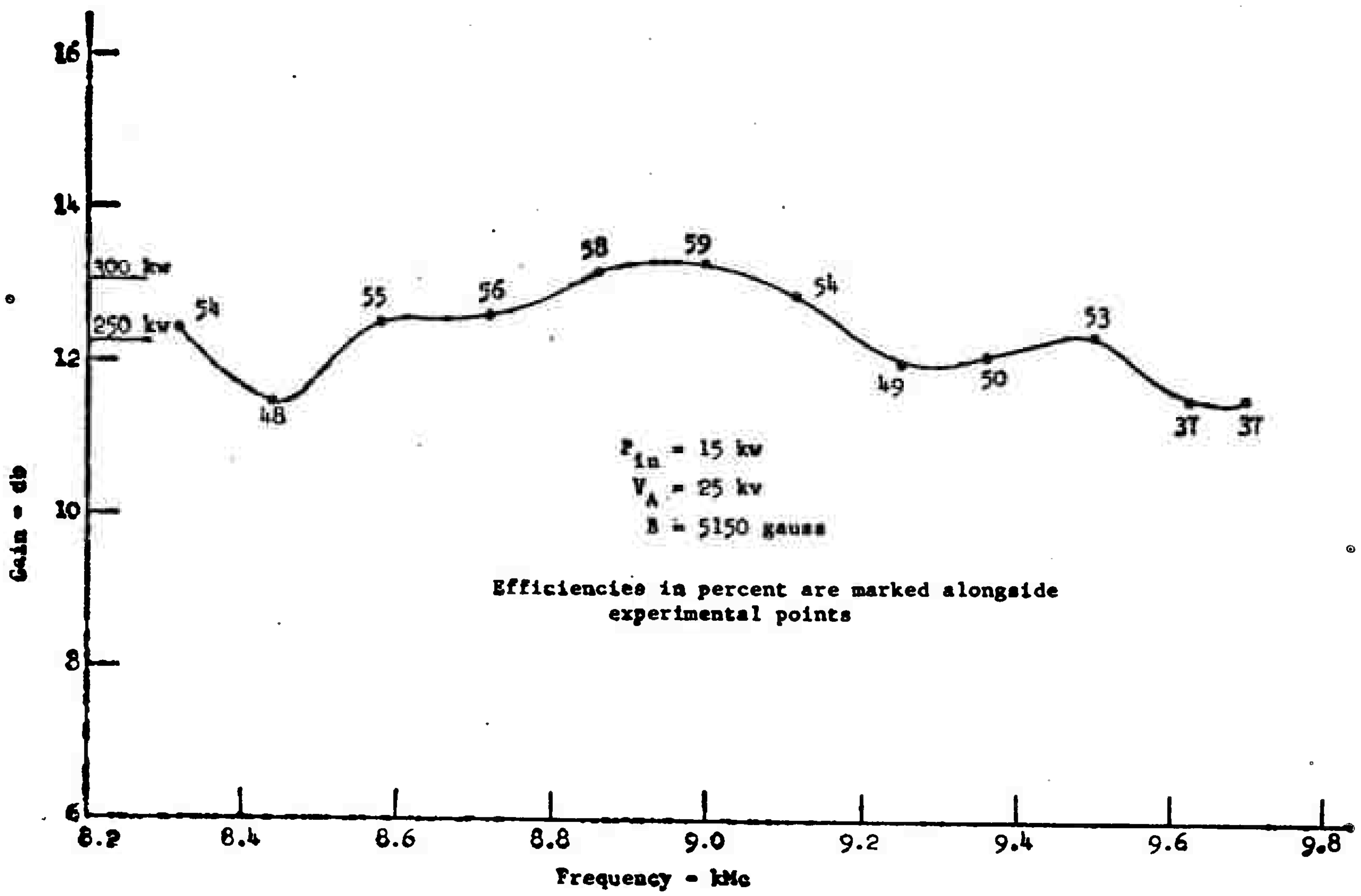

FIGURE 12 - GAIN AS A FUNCTION OF FREQUENCY FOR THE SFD-205

Efficiencies were quite good and are marked alongside the measured points. It is believed that with further effort, this gain can be raised to 15 db with comparable flatness.

Another gratifying result obtained with the SFD-205 is that the noise performance is much better than that of the SFD-202. With inputs as low as 10 kw the signal-to-spurious ratio appears to be greater than 30 db.

Thus, in spite of our problems, there are indications that the SFD-205 is capable of performing considerably better than the SFD-202.

5.2 The SFD-207

In the SFD-207 program, we have experienced the same problems with cathodes and multipactoring as in the SFD-205. These problems have prevented us from obtaining any extensive data on the tube. The data we have obtained indicate the tube has low gain - lower than we should expect from experience with a similar tube with fewer sections on a previous program. These results were presented on a V - I plot with power outputs and efficiencies marked alongside the experimental points. Gains in the 8 to 9 db range were obtained. We feel that there may be something wrong with this tube other than just cathode and multipactor troubles which explain its relatively poor performance.

As with the SFD-205, the signal-to-noise performance of the SFD-207 is much better than that of the SFD-202.

6.0 MULTIPACTOR EFFECTS

Attenuation of high power signals passed through our tubes by multipactor effects has been a continuing source of difficulty. These effects are particularly severe after a demountable tube has been operated, opened and rebuilt several times. Evidentally oxidation of the copper surfaces increases secondary emission ratio and enhances multipactor operation. When tube bodies which have been giving multipactor are passed through a hydrogen furnace the multipactoring is often completely eliminated for a while or at least much reduced.

The appearance of an RF pulse undergoing multipactor attenuation is sketched in Figure 13A. There is an initial spike of transmission after which the pulse "collapses". This effect can be observed with no voltage applied to the cathode and is not greatly affected when voltage is applied. A typical curve giving attenuation introduced by multipactoring as a function of magnetic field is shown in Figure 13B. At high magnetic fields there is no multipactoring. This indicates that the multipactor effect must be across magnetic field lines since multipactoring parallel to the magnetic field would not be eliminated by high field. On the other hand multipactor discharges between vane tips or between vane tips and cathode should not occur at the power levels employed (for magnetic fields of more than a few hundred gauss) because these discharges would be "cut-off" by the magnetic field turning the electron trajectories just as it does in normal crossed-field interaction. Further it would not be expected that such multipactor discharges would show maxima as a function of magnetic field as are observed. In some experiments, the cathode was completely removed from the tube and multipactoring continued. Thus we must look further for the cause of our multipactor.

A likely source for this multipactor effect is sketched in Figure 14. Electrons multipactor along the surfaces of the vanes being turned by the magnetic field so that they return to the vane from which they started. A continuous source of electrons at the starting point of

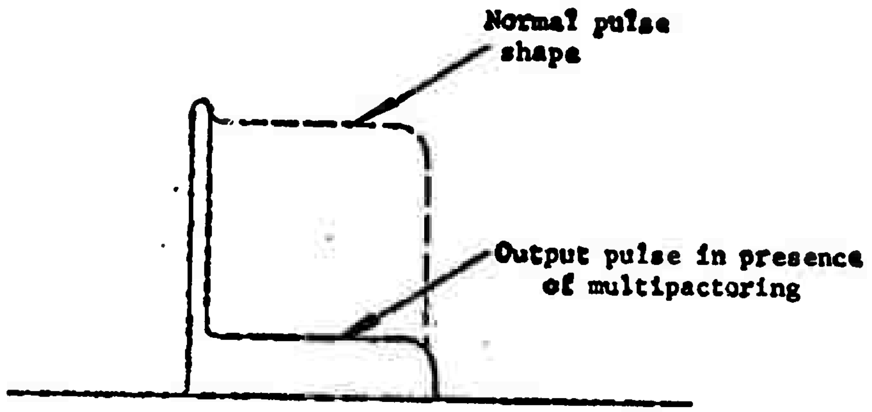

FIGURE 13A - OUTPUT PULSE SHAPE IN THE PRESENCE OF MULTIPACTOR ATTENUATION

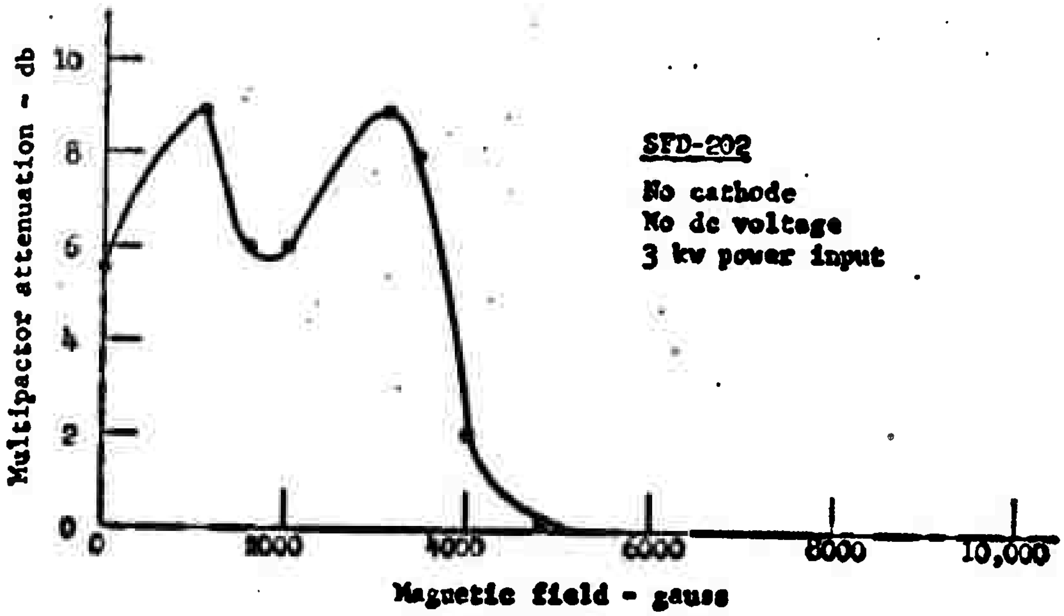

FIGURE 13B - MULTIPACTOR ATTENUATION AS A FUNCTION OF MAGNETIC FIELD IN THE SFD-202

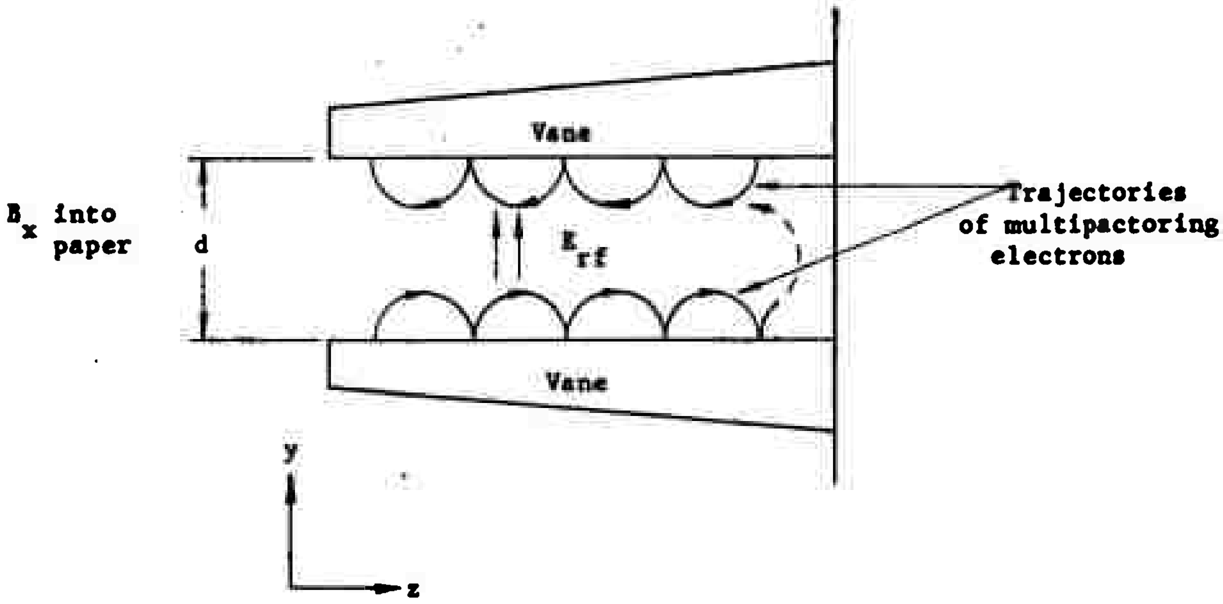

FIGURE 14 - SKETCH SHOWING POSTULATED MULTIPACTOR MECHANISM

the multipactor is provided either by electrons delivered by the multipactor discharge going in the opposite direction on the opposite vane or by electrons drifting back midway between vanes under the influence of space charge forces. It should be remembered that a comparatively small percentage feedback will be required to keep an effect of this nature going for even a moderate number of multiplication steps. There are also probably some electrons which remain in the space between RF pulses and assist in getting the discharge initiated in each RF pulse. This may be deduced from the fact that when RF input is first applied there is usually a delay of several seconds before the discharge will start. Once started, however, the multipactor occurs on every pulse and the starting time is measured in microseconds.

It will be noted that the mechanism postulated here is one that will be sensitive to magnetic field. It will give a maximum attenuation when the time required for an electron starting from the vane surface to return to the surface is just one RF cycle. We can set up the force equations and solve for this condition to see if it corresponds with the observed attenuation maxima. We can thus write, using the coordinate system of Figure 14

$$m \ddot{y} = e E \sin \omega t - e B \dot{x} \tag{1}$$

$$m \ddot{x} = e B \dot{y} \tag{2}$$

where e and m are the charge and mass of the electron, B is the magnetic field, E is the peak RF field, ω is the RF radian frequency and the dots indicate differentiation with respect to time.

Integrating (2), applying the boundary condition that at $y = 0$, $\dot{x} = \dot{y} = 0$ and substituting into (1), we find that

$$\ddot{y} + \omega_c^2 y = \eta E \sin \omega t \tag{3}$$

where $\eta = \frac{e}{m}$

$\omega_c = \eta B$

Solving this equation with the boundary conditions that exist when $t = 0$, then $y = z = \dot{y} = \dot{z} = 0$ we find

$$y = \left(\frac{\eta E}{\omega_c^2 - \omega^2}\right)\left(\sin \omega t - \frac{\omega}{\omega_c} \sin \omega_c t\right) \tag{4}$$

$$z = \left(\frac{\eta E}{\omega_c^2 - \omega^2}\right)\left(\frac{\omega}{\omega_c} \cos \omega_c t - \frac{\omega_c}{\omega} \cos \omega t\right) + \frac{\eta E}{\omega \omega_c} \tag{5}$$

A special situation is encountered when $\omega = \omega_c$. Then $\omega_c^2 - \omega^2 = 0$, and $(\sin \omega t - \omega/\omega_c \sin \omega_c t) = 0$ and the expression becomes indeterminant. To evaluate it at $\omega = \omega_c$, we write $\omega = \omega_c - \Delta$ and take the limit as $\Delta \rightarrow 0$. By this process we find

$$y = \frac{\eta E}{2\omega_c^2} (\sin \omega_c t - \omega_c t \cos \omega_c t) \tag{6}$$

$$z = \frac{\eta E}{2\omega_c^2} (1 - \cos \omega_c t - \omega_c t \sin \omega_c t) \tag{7}$$

The condition for a multipactor resonance is that y return to zero when $\omega t = 2\pi$. Applying this in (4), we find that this occurs for

$$\frac{\omega_c}{\omega} = \frac{n}{2} \quad \text{where } n = 1, 3, 4, 5, \text{ etc.}$$

i.e., all integers except 2. Equation (6) shows that when $n = 2$ $(\omega_c = \omega)$, the resonance condition is not satisfied. Therefore, the analysis predicts resonances when the magnetic field is 1/2, 3/2, 4/2, etc. of the cyclotron resonance field. Actually we obtain only two maxima of attenuation as shown in Figure 13B. The magnetic field at these attenuation maxima are, however, very close to the predicted values as shown in Figure 15, where we plot magnetic field for maximum attenuation as a function of frequency. The higher n mode attenuations may in principle exist but may never get started.

We can find the striking energy from

$$\dot{y} = \left(\frac{\omega \eta E}{\omega_c^2 - \omega^2}\right)(\cos \omega t - \cos \omega_c t) \tag{8}$$

When $\omega t = 2\pi$ and $\omega_c = 1.5\,\omega$, this gives

$$\dot{y} = 1.2\,\frac{E}{B}$$

Using an estimated value of E for our SFD-202 circuit with an input power of 1 kw, we estimate the striking energy to be of the order of 30 to 50 volts. This would not be enough to get the secondary emission ratio greater than unity when the surface is clean copper. It may, however, be adequate if the surface is covered by an oxide layer. This result thus also corresponds to our experience that clean tubes do not multipactor. The evidence seems pretty strong that the effect postulated is the one we are observing - at least at high magnetic fields where the multipactor is of importance.

At zero or at low magnetic field, there may be multipactors between vane tips or between vanes and cathode. If the tube is allowed to multipactor at zero field, an electron current of the order of a few tens of microamperes is drawn to the cathode and to the insulated pole piece. Whether this is evidence of a multipactor between these electrodes and vanes or whether these are just stray electrons is not known. As

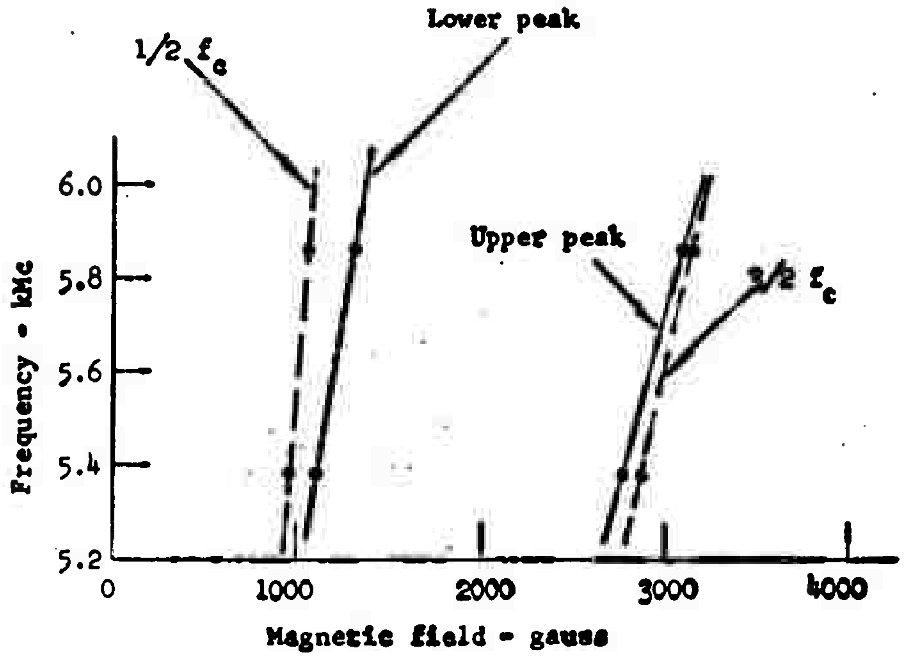

FIGURE 15 - MAGNETIC FIELD FOR MAXIMUM MULTIPACTOR ATTENUATION AS A FUNCTION OF FREQUENCY COMPARED WITH $f_c/2$ AND $3f_c/2$

magnetic field is increased, these currents go through several maxima and minima and then disappear. At high magnetic fields near the operating values for the tube, no currents are drawn by the multipactor effect.

7.0 SLOW-WAVE CIRCUIT STUDIES

Experiments were made during the last quarter to see if the C_{13} couplers could be lifted off the bars of the circuit of a tube such as the SFD-203 and connected to the back wall. For this purpose an experiment was made using an array of bars with projections from a back wall coupling capacitively to the bars. There were two rows of such projections. One row coupled to every alternate bar and the other row coupled to those bars not coupled to the first row in a manner analogous to how we make rows of C_{13} couplers in the SFD-203.

Results of cold tests on this circuit showed that it operates quite differently from a normal C_{13} circuit. Evidentally propagation occurs at low phase shift per section and the circuit is not materially different from a Karp circuit. For our purposes this removes it from the area of interest.

8.0 CATHODE STUDIES

As mentioned in connection with our X-band studies, we found that beryllium copper cathodes will deactivate when arcing takes place in a tube. After arcing considerably less current can be drawn than before arcing. The deactivation shows up as the appearance of a maximum current boundary phenomenon. This is shown by Figure 16 which is a plot of anode current as a function of the ratio of magnetic field to the cut-off magnetic field for a tube in which deactivation has occurred. As magnetic field is lowered the current increases until a maximum value of about 13 peak amperes is reached. The current then suddenly drops to a low value. Thus, a horizontal line at 13 amps represents a maximum current boundary. It is to be noted that the shape of this boundary is much different than that shown in Figure 3 for a small diameter smooth-bore tube.

Prior to deactivation, this cathode could draw a considerably larger current. This is indicated by the dotted lines in Figure 16. At B/B_{co} of 1.15, a current of 70 amps was obtained. The appearance of a maximum current boundary does not affect the current drawn if this current is moderately less than the boundary value. In such a range, the tube is operating space charge limited and operation is not affected by cathode properties. When the boundary is reached, the tube tries to draw more current than the cathode can supply. What possibly happens is that the hub space charge is rapidly decreased and cathode back bombardment is reduced until it can no longer supply the current called for. This reduction in back bombardment would account for the current dropping to a low value rather than just limiting at the maximum value.

A very similar deactivation to that depicted in Figure 16 for the SFD-205 has also been observed in the SFD-207 and on rare occasions in the SFD-202.

One cure for this difficulty is to use spacings large enough so that arcing does not occur. This may, however, be difficult at X-band

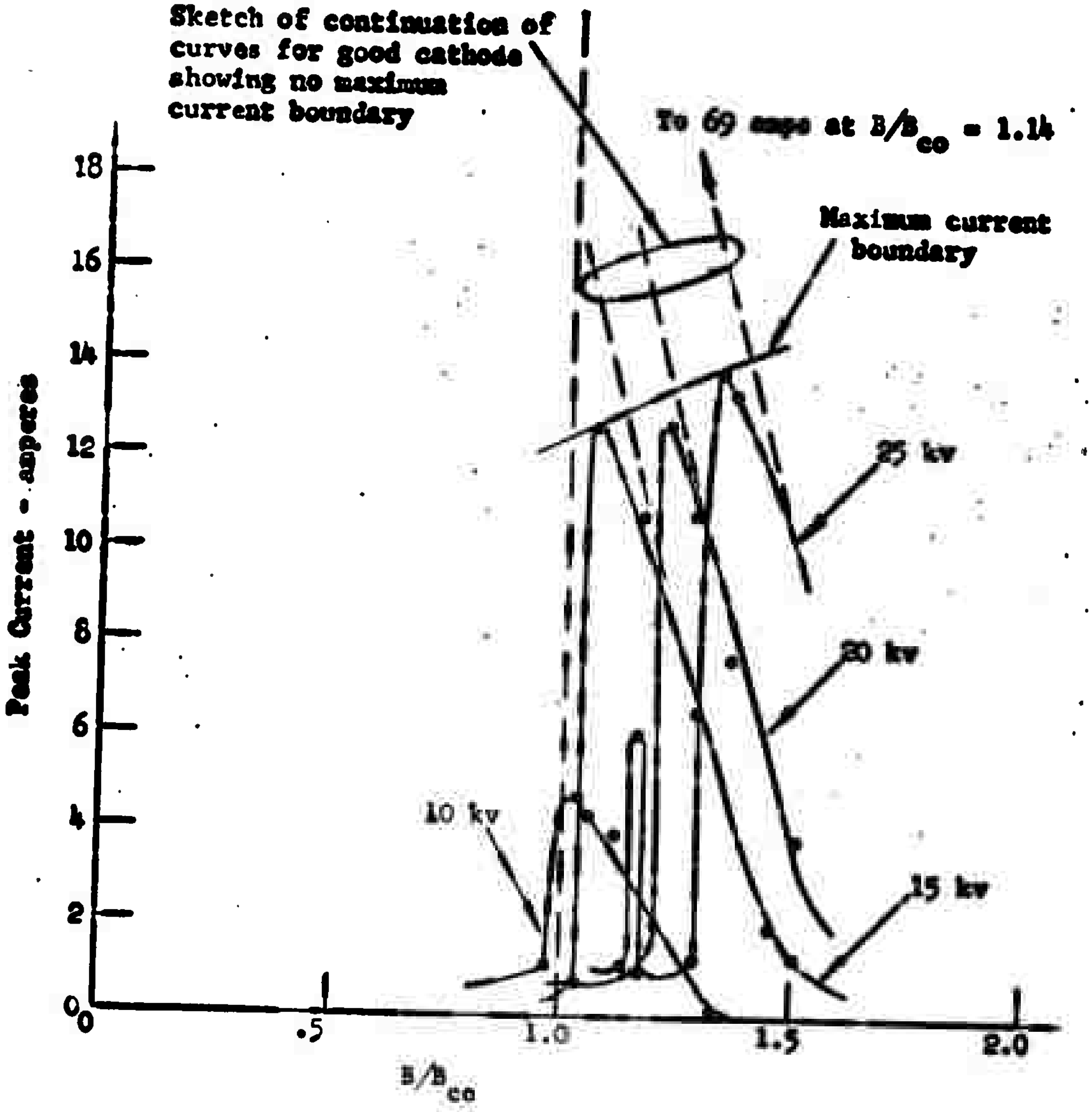

FIGURE 16 - CURRENT AS A FUNCTION OF B/B$_{co}$ FOR SFD-205 AFTER CATHODE DEACTIVATION BY ARCING. CURVES SHOW APPEARANCE OF MAXIMUM CURRENT BOUNDARY PHENOMENON

so that another cure must be looked for. A likely possibility is the use of an oxide impregnated nickel matrix cathode as is used in magnetrons. Such cathodes appear to be less sensitive to deactivation caused by arcing. For use in a tube operating from a dc voltage such a cathode must be kept cool so that there is no primary emission which could cause noise or spurious turn-on in the interpulse period. Such an oxide cathode has been tried recently in an SFD-202 tube. The cathode was constructed on a solid cylinder and no heater was used. The cathode was activated by heating it in a bell jar to break down the carbonates. It was then removed from the bell jar and placed in the tube. When the tube was first tested, it gave off more gas for a few hours than did a tube with a beryllium copper cathode but then settled down to operate at the same low pressure. The current drawn from the oxide cathode was substantially the same as that from a beryllium copper cathode as shown in the curves of Figure 12 of the second quarterly report. The next step will be to incorporate such a cathode in the X-band tubes.

We can show the factors that the maximum current boundary depends on by the following procedure. The ratio of hub thickness to the anode-to-cathode spacing is given by

$$\frac{y}{d} = \frac{2}{\frac{V}{V_o} + 1} \approx \frac{2}{\frac{V}{V_o}} \qquad (1)$$

or

$$\frac{y}{d} \sim \frac{V_o}{V} \quad \text{approximately}$$

where
- y = the hub thickness
- d = the anode-to-cathode spacing
- V = the anode voltage
- V_o = the synchronous voltage

The average charge density in the hub is given by

$$\rho = \eta \, \epsilon_o \, B^2 \qquad (2)$$

The time for an electron to complete a trajectory leaving the cathode and later returning to the cathode is shown by Slater to be proportional to $1/\omega_c$ for a striated solution of the hub space charge. We will assume that the effects of RF represent a perturbation of such a trajectory so that the same proportionality to $1/\omega_c$ will hold. From this, we can calculate that the current returning to the cathode will be proportional to ω_c times the total charge in the hub.

$$I_r \sim B^3 \, h \, r \, d \left(\frac{V_o}{V}\right) \qquad (3)$$

where I_r = the current returning to the cathode
h = the cathode height
r = the radius
B = magnetic field

The current available to be drawn from the cathode must be δ times I_r, where δ is the secondary emission ratio. Of this current $(\delta - 1)\, I_r$ is available to be drawn to the anode while I_r must return to the cathode to maintain the back bombardment. Thus the current available to be drawn to the anode becomes

$$I \sim (\delta - 1) \, B^3 \, h \, r \, d \, \frac{V_o}{V} \qquad (4)$$

Using v_o, the synchronous velocity $\approx \frac{V}{Bd}$ we obtain

$$I \sim (\delta - 1) \, B^2 \, h \, r \, V_o^{1/2} \qquad (5)$$

However, $B^2 \, h \, r \, V_o^{1/2}$ is proportional to the characteristic current.

Thus, we come to the conclusion the maximum available current is proportional to $(\delta - 1)$ times the characteristic current. Since all tubes of a given class tend to operate at the same ratio of current to characteristic current, the limitations imposed by a maximum current boundary are a function of $(\delta - 1)$ alone. A low δ would be just as much of a problem in a low frequency tube as in a high frequency one even though the current density drawn in the former was very much less.

9.0 CONCLUSIONS

The conclusions to be drawn from the work done this quarter are:

1. Crossed-field amplifiers can be constructed with bandwidths of 8 to 12% with the tube operating at constant anode voltage. The frequency response curve is determined by counteracting tendencies of the rate of field decay away from the anode surface and the percentage of voltage above the Hartree value. A gain of 12 ± 0.75 db has been obtained with this type of operations. Gains of 17 db have been obtained at spot points without a simultaneous investigation of the gain vs. frequency characteristic.

2. The frequencies of smooth-bore or space charge modes are determined by resonances of the interaction space, not by any characteristic of the mode itself.

3. Turn-off with a control electrode can be obtained with a geometry which is compatible with our usual techniques for debunching spokes in the drift region.

4. A method of determining leakage current to the pole pieces has been worked out and applied to the SFD-202 tube. The same technique can later be applied to other tubes. Tests have shown that leakage current in the SFD-202 is small and that space charge mode current goes across the interaction space to the anode.

5. A multipactor effect in which electrons run along the sides of the vanes is responsible for attenuation effects observed when the magnetic field is close to the operating value. Such multipactor effects can be avoided by keeping the surfaces clean.

6. Arcing in a tube causes deactivation of beryllium copper cathodes. The deactivation shows up as a maximum current boundary. For currents less than the maximum, the tube operates space charge limited and operation is independent of cathode properties. When the maximum current is exceeded the current suddenly drops to a low value.

7. Secondary emitting cathodes can be made by the normal techniques used for magnetrons except that the heater is omitted. The cathode may be activated in a bell jar and later placed in the tube.

8. Cold tests of the complete SFD-203 tube have turned up no fundamental problems. We will now proceed to hot test the tube. Some resonances in the tube body have been found which will have to be eliminated eventually but chances are that they will not interfere with initial hot testing at selected points in the band.

10.0 PROGRAM FOR NEXT QUARTER

1. Hot test the SFD-203 tube.

2. Continue tests with the SFD-202 smooth-bore tube for the purpose of better understanding of space charge modes.

3. Continue tests on control electrode in the SFD-202 tube.

4. Continue experiments on the two X-band tubes. Incorporate oxide cathodes into these tubes. Compare operation of forward and backward wave tubes. See how much gain can be obtained at constant voltage in the forward wave tube.

5. Initiate tests of secondary emission of cathodes using a secondary emission tester.

LIST OF REFERENCES

1. Pierce, J. R., TRAVELING WAVE TUBES, D. Van Nostrand, 1950, page 96

2. Bunemann, O., "A Small Amplitude Theory for Magnetrons," Journal of Electronics and Control, July 1957

3. Slater, John C., MICROWAVE ELECTRONICS, D. Van Nostrand, 1950, page 336

DISTRIBUTION LIST

	Copies
OASD (R & E), Rm 3E1065 The Pentagon Attn: Technical Library Washington 25, D. C.	1
Chief, Research and Development OCS, Dept. of the Army Washington 25, D. C.	1
Chief Signal Officer Attn: SIGRD Department of the Army Washington 25, D. C.	1
Director U. S. Naval Research Laboratory Attn: Code 2027 Washington 25, D. C.	1
Commanding Officer and Director U. S. Navy Electronics Laboratory San Diego 52, California	1
Commander Air Systems Division Attn: ASWRNET Wright-Patterson AFB, Ohio	2
Commander Electronics Systems Division Attn: ESRRI Bedford, Massachusetts	1
Commander Rome Air Development Center Attn: RCOIL-2 Griffiss Air Force Base, New York	1
Commander Armed Services Technical Information Agency Attn: TIPCR Arlington Hall Station Arlington 12, Virginia	10
Chief, Army Research Office Washington 25, D. C.	1

DISTRIBUTION LIST - continued

	Copies
Commanding Officer U. S. Army Signal Research & Development Laboratory Attn: SIGRA/SL-PRM (Records File Copy) Fort Monmouth, New Jersey	1
Commanding Officer U. S. Army Signal Research & Development Laboratory Attn: Technical Information Division Fort Monmouth, New Jersey	5
Advisory Group on Electron Tubes 346 Broadway New York 13, New York	2
Commanding Officer Frankford Arsenal Attn: ORDBA-FEL Philadelphia 37, Pennsylvania	1
Chief of Ordnance Attn: ORDTX-AR Washington 25, D. C.	1
Chief, Bureau of Ships Attn: Code 691A (LCDR) Mr. J. F. DeBold Department of the Navy Washington 25, D. C.	1
Commanding General Attn: Technical Library Redstone Arsenal, Alabama	1
Director, USAF Project Rand Air Force Liaison Office The Rand Corporation 1700 Main Street Santa Monica, California	1
Varian Associates 611 Hansen Way Palo Alto, California Attn: Mr. T. Moreno	1
Sperry Gyroscope Co. Division of Sperry Rand Corporation Great Neck, Long Island, New York Attn: Dr. V. R. Learned	1

DISTRIBUTION LIST - continued

	Copies
Commanding Officer Diamond Ordnance Fuze Laboratories Attn: Library, Rm. 211, Bldg. 92 Washington 25, D. C.	1
Commanding Officer, 9560th TSU U. S. Army Signal Electronics Research Unit P. O. Box 205 Mountain View, California	1
Chief, U. S. Army Security Agency Arlington Hall Station Arlington 12, Virginia	2
Deputy President U. S. Army Security Agency Board Arlington Hall Station Arlington 12, Virginia	1
Commanding Officer U. S. Army Signal Material Support Agency Attn: SIGMS-ADJ Fort Monmouth, New Jersey	1
Corps of Engineers Liaison Office U. S. Army Signal Research & Development Laboratory Fort Monmouth, New Jersey	1
U. S. Navy Electronics Liaison Office U. S. Army Signal Research & Development Laboratory Fort Monmouth, New Jersey	1
Marine Corps Liaison Office U. S. Army Signal Research & Development Laboratory Fort Monmouth, New Jersey	1
Commanding Officer U. S. Army Signal Research & Development Laboratory Attn: Logistics Division (For SIGRA/SL-PRM) (Project Engineer) Fort Monmouth, New Jersey	2
Commanding Officer U. S. Army Signal Research & Development Laboratory Attn: Director of Research Fort Monmouth, New Jersey	1

DISTRIBUTION LIST - continued

	Copies
Commanding Officer U. S. Army Signal Research & Development Laboratory Attn: Technical Documents Center Fort Monmouth, New Jersey	1
ARGMA Liaison Officer Bell Telephone Laboratories Attn: Lt. Col. Lee G. Jones Whippany, New Jersey	1
Commander Army Rocket and Guided Missile Agency Attn: ORDXR-RMP Redstone Arsenal, Alabama	1
Raytheon Manufacturing Company Waltham, Massachusetts Attn: Mr. William C. Brown	1
Commander Air Force System Command Attn: SCRC (Capt. C. Zimmerman) Andrews Air Force Base Washington 25, D. C.	1
Litton Industries 960 Industrial Road San Carlos, California Attn: Dr. G. E. Pokorney	1
Raytheon Company Microwave & Power Tube Division Spencer Laboratory Wayside Avenue Burlington, Massachusetts Attn: Librarian	1
Director, Lincoln Laboratory Attn: Dr. L. Huernsey P. O. Box 73 Lexington 73, Massachusetts	1
Director of Defense Research & Engineering Attn: Mr. James M. Bridges Washington 25, D. C.	1

DISTRIBUTION LIST - continued

	Copies
Aerospace Corporation Attn: Dr. I. Getting Los Angeles 45, California	1
Chief of Naval Research Department of the Navy Attn: Code 461 Washington 25, D. C.	1
Chief, Bureau of Naval Weapons Department of the Navy Attn: Code RAAD-4423	1
Attn: Code 691A4	1
Washington 25, D. C.	
Commander, Air Force Ballistic Missile Division Attn: WDZRS Air Force Unit Post Office Los Angeles 45, California	1
Commanding Officer U. S. Army Signal Research & Development Laboratory Fort Monmouth, New Jersey Attn: SIGRA/SL-PR	1
SIGRA/SL-SR	1
SIGRA/SL-SC	1
SIGRA/SL-PE	1
SIGRA/SL-N	1

This contract is supervised by the Microwave Tubes Branch, USASRDL, Fort Monmouth, New Jersey. For further technical information, contact Mr. J. D'Andrea, Project Engineer, Telephone 59-61104.

AD ______________________

S-F-D laboratories, inc., Union, New Jersey, RESEARCH ON SUPER POWER MICROWAVE AMPLIFIERS, by N. L. McDowell, July 1961, Report No. 4, 48 pp. inc. illus. (Task No. 3A99-13-001-C5)

During this quarter construction of the first SFD-203 tube has been completed. The tube is now being pumped. Experiments on the SFD-202 and SFD-205 have shown that frequency responses flat over 8 - 12% bandwidth can be obtained with constant anode voltage. Experiments on a smooth-bore tube have shown that the frequencies of the space charge mode are largely determined by a coaxial line resonance of the stem. Experiments on the SFD-202 have shown that control electrode turn-off can be accomplished with a geometry which is compatible with our usual techniques for debunching spokes in the drift region.

UNCLASSIFIED

1. Introduction
2. The SFD-203 Program
3. Smooth Bore Experiments
4. The SFD-202 Program
5. The X-band Program
6. Multipactor Effects
7. Slow-wave Circuit Studies
8. Cathode Studies
9. Conclusions
10. Program for Next Quarter
I. H. L. McDowell

UNCLASSIFIED

AD ______________________

S-F-D laboratories, inc., Union, New Jersey, RESEARCH ON SUPER POWER MICROWAVE AMPLIFIERS, by H. L. McDowell, July 1961, Report No. 4, 48 pp. inc. illus. (Task No. 3A99-13-001-05)

During this quarter construction of the first SFD-203 tube has been completed. The tube is now being pumped. Experiments on the SFD-202 and SFD-205 have shown that frequency responses flat over 8 - 12% bandwidth can be obtained with constant anode voltage. Experiments on a smooth-bore tube have shown that the frequencies of the space charge mode are largely determined by a coaxial line resonance of the stem. Experiments on the SFD-202 have shown that control electrode turn-off can be accomplished with a geometry which is compatible with our usual techniques for debunching spokes in the drift region.

UNCLASSIFIED

1. Introduction
2. The SFD-203 Program
3. Smooth Bore Experiments
4. The SFD-202 Program
5. The X-bend Program
6. Multipactor Effects
7. Slow-wave Circuit Studies
8. Cathode Studies
9. Conclusions
10. Program for Next Quarter
I. H. L. McDowell

UNCLASSIFIED

AD ______________________

S-F-D laboratories, inc., Union, New Jersey, RESEARCH ON SUPER POWER MICROWAVE AMPLIFIERS, by H. L. McDowell, July 1961, Report No. 4, 48 pp. inc. illus. (Task No. 3A99-13-001-05)

During this quarter construction of the first SFD-203 tube has been completed. The tube is now being pumped. Experiments on the SFD-202 and SFD-205 have shown that frequency responses flat over 8 - 12% bandwidth can be obtained with constant anode voltage. Experimeots on a smooth-bore tube have shown that the frequencies of the space charge mode are largely determined by a coaxial line resonance of the stem. Experiments on the SFD-202 have shown that control electrode turn-off can be accomplished with a geometry which is compatible with our usual techniques for debunching spokes in the drift region.

UNCLASSIFIED

1. Introduction
2. The SFD-203 Program
3. Smooth Bore Experiments
4. The SFD-202 Program
5. The X-band Program
6. Multipactor Effects
7. Slow-wave Circuit Studies
8. Cathode Studies
9. Conclusions
10. Program for Next Quarter
I. N. L. McDowell

UNCLASSIFIED

AD ______________________

S-F-D laboratories, inc., Union, New Jersey, RESEARCH ON SUPER POWER MICROWAVE AMPLIFIERS, by N. L. McDowell, July 1961, Report No. 4, 48 pp. inc. illus. (Task No. 3A99-13-001-05)

During this quarter construction of the first SFD-203 tube has been completed. The tube is now being pumped. Experiments on the SFD-202 and SFD-205 have shown that frequency responses flat over 8 - 12% bandwidth can be obtained with constant anode voltage. Experiments on a smooth-bore tube have shown that the frequencies of the space charge mode are largely determined by a coaxial line resonance of the stem. Experiments on the SFD-202 have shown that control electrode turn-off can be accomplished with a geometry which is compatible with our usual techniques for debunching spokes in the drift region.

UNCLASSIFIED

1. Introduction
2. The SFD-203 Program
3. Smooth Bore Experiments
4. The SFD-202 Program
5. The X-bend Program
6. Multipactor Effects
7. Slow-wave Circuit Studies
8. Cathode Studies
9. Conclusions
10. Program for Next Quarter
I. H. L. McDowell

UNCLASSIFIED

AD ____________________

S-F-D laboratories, inc., Union, New Jersey, **RESEARCH ON SUPER POWER MICROWAVE AMPLIFIERS**, by H. L. McDowell, July 1961, Report No. 4, 48 pp. inc. illus. (Task No. 3A99-13-001-05)

During this quarter construction of the first SFD-203 tube has been completed. The tube is now being pumped. Experiments on the SFD-202 and SFD-205 have shown that frequency responses flat over 8 - 12% bandwidth can be obtained with constant anode voltage. Experiments on a smooth-bore tube have shown that the frequencies of the space charge mode are largely determined by a coaxial line resonance of the stem. Experiments on the SFD-202 have shown that control electrode turn-off can be accomplished with a geometry which is compatible with our usual techniques for debunching spokes in the drift region.

UNCLASSIFIED

1. Introduction
2. The SFD-203 Program
3. Smooth Bore Experiments
4. The SFD-202 Program
5. The X-band Program
6. Multipactor Effects
7. Slow-wave Circuit Studies
8. Cathode Studies
9. Conclusions
10. Program for Next Quarter

I. H. L. McDowell

UNCLASSIFIED

AD ____________________

S-F-D laboratories, inc., Union, New Jersey, **RESEARCH ON SUPER POWER MICROWAVE AMPLIFIERS**, by H. L. McDowell, July 1961, Report No. 4, 48 pp. inc. illus. (Task No. 3A99-13-001-05)

During this quarter construction of the first SFD-203 tube has been completed. The tube is now being pumped. Experiments on the SFD-202 and SFD-205 have shown that frequency responses flat over 8 - 12% bandwidth can be obtained with constant anode voltage. Experiments on a smooth-bore tube have shown that the frequencies of the space charge mode are largely determined by a coaxial line resonance of the stem. Experiments on the SFD-202 have shown that control electrode turn-off can be accomplished with a geometry which is compatible with our usual techniques for debunching spokes in the drift region.

UNCLASSIFIED

1. Introduction
2. The SFD-203 Program
3. Smooth Bore Experiments
4. The SFD-202 Program
5. The X-band Program
6. Multipactor Effects
7. Slow-wave Circuit Studies
8. Cathode Studies
9. Conclusions
10. Program for Next Quarter

I. H. L. McDowell

UNCLASSIFIED

AD ____________________

S-F-D laboratories, inc., Union, New Jersey, **RESEARCH ON SUPER POWER MICROWAVE AMPLIFIERS**, by H. L. McDowell, July 1961, Report No. 4, 48 pp. inc. illus. (Task No. 3A99-13-001-05)

During this quarter construction of the first SFD-203 tube has been completed. The tube is now being pumped. Experiments on the SFD-202 and SFD-205 have shown that frequency responses flat over 8 - 12% bandwidth can be obtained with constant anode voltage. Experiments on a smooth-bore tube have shown that the frequencies of the space charge mode are largely determined by a coaxial line resonance of the stem. Experiments on the SFD-202 have shown that control electrode turn-off can be accomplished with a geometry which is compatible with our usual techniques for debunching spokes in the drift region.

UNCLASSIFIED

1. Introduction
2. The SFD-203 Program
3. Smooth Bore Experiments
4. The SFD-202 Program
5. The X-band Program
6. Multipactor Effects
7. Slow-wave Circuit Studies
8. Cathode Studies
9. Conclusions
10. Program for Next Quarter

I. H. L. McDowell

UNCLASSIFIED

AD ____________________

S-F-D laboratories, inc., Union, New Jersey, **RESEARCH ON SUPER POWER MICROWAVE AMPLIFIERS**, by H. L. McDowell, July 1961, Report No. 4, 48 pp. inc. illus. (Task No. 3A99-13-001-05)

During this quarter construction of the first SFD-203 tube has been completed. The tube is now being pumped. Experiments on the SFD-202 and SFD-205 have shown that frequency responses flat over 8 - 12% bandwidth can be obtained with constant anode voltage. Experiments on a smooth-bore tube have shown that the frequencies of the space charge mode are largely determined by a coaxial line resonance of the stem. Experiments on the SFD-202 have shown that control electrode turn-off can be accomplished with a geometry which is compatible with our usual techniques for debunching spokes in the drift region.

UNCLASSIFIED

1. Introduction
2. The SFD-203 Program
3. Smooth Bore Experiments
4. The SFD-202 Program
5. The X-band Program
6. Multipactor Effects
7. Slow-wave Circuit Studies
8. Cathode Studies
9. Conclusions
10. Program for Next Quarter

I. H. L. McDowell

UNCLASSIFIED

UNCLASSIFIED

UNCLASSIFIED